Coagulation factors directly cleave SARS-CoV-2 spike and enhance viral entry.

Edward R. Kastenhuber[1], Javier A. Jaimes[2], Jared L. Johnson[1], Marisa Mercadante[1], Frauke Muecksch[3], Yiska Weisblum[3], Yaron Bram[4], Robert E. Schwartz[4,5], Gary R. Whittaker[2] and Lewis C. Cantley[1,*]

Affiliations

1. Meyer Cancer Center, Department of Medicine, Weill Cornell Medical College, New York, NY, USA.
2. Department of Microbiology and Immunology, Cornell University, Ithaca, New York, USA.
3. Laboratory of Retrovirology, The Rockefeller University, New York, NY, USA.
4. Division of Gastroenterology and Hepatology, Department of Medicine, Weill Cornell Medicine, New York, NY, USA.
5. Department of Physiology, Biophysics and Systems Biology, Weill Cornell Medicine, New York, NY, USA.

*Correspondence: lcantley@med.cornell.edu

Summary

Coagulopathy is recognized as a significant aspect of morbidity in COVID-19 patients. The clotting cascade is propagated by a series of proteases, including factor Xa and thrombin. Other host proteases, including TMPRSS2, are recognized to be important for cleavage activation of SARS-CoV-2 spike to promote viral entry. Using biochemical and cell-based assays, we demonstrate that factor Xa and thrombin can also directly cleave SARS-CoV-2 spike, enhancing viral entry. A drug-repurposing screen identified a subset of protease inhibitors that promiscuously inhibited spike cleavage by both transmembrane serine proteases as well as coagulation factors. The mechanism of the protease inhibitors nafamostat and camostat extend beyond inhibition of TMPRSS2 to coagulation-induced spike cleavage. Anticoagulation is critical in the management of COVID-19, and early intervention could provide collateral benefit by suppressing SARS-CoV-2 viral entry. We propose a model of positive feedback whereby infection-induced hypercoagulation exacerbates SARS-CoV-2 infectivity.

Keywords:

SARS-CoV-2, COVID-19, coronavirus, entry, factor Xa, thrombin, coagulopathy, anticoagulants, camostat, nafamostat,

Introduction

SARS-CoV-2 emerged into the human population in late 2019 and has evolved into a devastating global health crisis. Extensive efforts to repurpose drugs and develop novel antiviral strategies have produced limited clinical results to date (Consortium et al., 2020). Despite the recent success of vaccine approaches (Baden et al., 2020; Polack et al., 2020), numerous challenges remain ahead and diversified, long term efforts to develop coronavirus antivirals are urgently needed. Logistical, geopolitical, and socioeconomic factors hinder the expediency and breadth of vaccine distribution (Kwok et al., 2020; Lin et al., 2020; Nhamo et al., 2020; So and Woo, 2020). By carrying a large reservoir of active cases over a long period of time, viral variants are emerging, threatening to decrease the efficiency of vaccine-induced immunity (Wang et al., 2021; Weisblum et al., 2020). Zoonotic outbreaks of SARS-like coronaviruses, which have already occurred three times in the last 20 years, continue to present a major global health concern in the future (Cheng et al., 2007; Ge et al., 2013; Menachery et al., 2015).

Coronaviruses attach to target cells via interactions with specific receptors and proteolytic processing of the spike protein by host cell proteases is required to facilitate membrane fusion and viral entry (Glowacka et al., 2011; Jaimes et al., 2020c; Walls et al., 2020), representing a potentially druggable vulnerability in the viral replication cycle. In SARS-CoV-2, as in SARS-CoV and MERS-CoV, host cell proteases act on two sites residing at the S1/S2 subunit boundary and at the S2' region proximal to the fusion peptide (Belouzard et al., 2009; Hoffmann et al., 2020a; Jaimes et al., 2020a; Millet and Whittaker, 2014). S1/S2 site cleavage opens up the spike trimer and exposes the S2' site, which must be cleaved to allow for the release of the fusion peptide (Benton et al., 2020). Deletion of the S1/S2 site attenuates SARS-CoV-2 *in vivo* (Johnson et al., 2021).

TMPRSS2, and other transmembrane serine proteases (TTSPs), are important host cell factors in proteolytic activation across multiple coronaviruses (Hoffmann et al., 2020a; Jaimes et al., 2019; Ou et al., 2020). TMPRSS2 has been validated genetically and pharmacologically *in vivo*, using mouse-adapted SARS-CoV in wild type mice and MERS-CoV in huDPP4-transgenic mice (Iwata-Yoshikawa et al., 2019; Zhou et al., 2015). More recently, TMPRSS2 has been highlighted as a promising antiviral drug target for SARS-CoV-2 (Hoffmann et al., 2020a; Hoffmann et al., 2020c). Two broad spectrum protease inhibitors with activity against TMPRSS2, Camostat and Nafamostat, have been clinically approved for other applications in Japan, but are not currently FDA-approved for any indication in the US.

Cathepsin L can cleave SARS-CoV spike at an alternative cleavage site during entry through the endosomal pathway of entry (Bosch et al., 2008), bypassing proteolysis at the cell surface by TTSPs (Simmons et al., 2011). Drug repurposing efforts for SARS-CoV-2 have identified hits targeting the endosomal cathepsins (Riva et al., 2020), but targeting the endosomal pathway only reduces infection in cell lines lacking TMPRSS2 and is ineffective *in vivo* (Bertram et al., 2013; Hoffmann et al., 2020a; Hoffmann et al., 2020b; Kleine-Weber et al., 2018; Shirato et al., 2017; Zhou et al., 2015).

While it has been suggested that furin cleaves the S1/S2 site and TMPRSS2 cleaves the S2' site (Bestle et al., 2020), our results question whether this division of labor is straightforward. Broad-spectrum protease inhibitors, but not furin-specific inhibitors, reduce infectivity in a cell-type-specific manner (Tang et al., 2021). Proteolytic activation of envelope proteins is a common feature of many viruses, presumably coordinating target cell engagement and envelope conformational changes leading to fusion. Complete furin cleavage during viral biogenesis, before release of viral particles, may render SARS-CoV-2 spike less stable in solution and reduce the likelihood to reach and interact with target cells (Amanat et al., 2021; Berger and Schaffitzel, 2020). Although the S1/S2 site is often referred to as the "furin site" (Johnson et al., 2021), the spectrum of proteases that actually catalyze the majority of biologically relevant activity in the lung remains undefined.

Comorbidities associated with more severe COVID-19 include cardiovascular disease, hypertension, and diabetes mellitus, which are also linked to dysregulated blood clotting (Zhou et al., 2020). Likewise, patients with a history of stroke prior to infection were nearly twice as likely to experience acute respiratory distress syndrome (ARDS) and in-hospital mortality (Qin et al., 2020).

Early in the course of disease, elevated D-dimer levels (an indicator of fibrinolysis and coagulopathy) measured upon initial hospital admission are a predictive biomarker of severe disease and lethality in COVID-19 patients (Zhou et al., 2020). Low platelet counts (an indicator of consumptive coagulopathy) were detected in 20% of patients who died in hospital compared to 1% of recovered cases (Zhou et al., 2020). Systemic activity of clotting factors V, VIII, and X are elevated in severe COVID-19 disease (Stefely et al., 2020).

The pathogenesis of SARS-CoV-2 infection has been associated with coagulopathy and thromboembolic events. Specifically, COVID-19 patients face elevated risk of pulmonary embolism and venous, arterial, and microvascular thrombosis (Huang et al., 2020; Kipshidze et al., 2020). While early phase disease is typically restricted to local pulmonary hypercoagulable

state, severe late stage disease may be accompanied by systemic disseminated intravascular coagulation (McGonagle et al., 2020), stroke and cardio-embolism (Tsivgoulis et al., 2020), reminiscent of SARS (Hwang et al., 2005; Umapathi et al., 2004). Ischemic stroke occurred in approximately 1% of hospitalized COVID-19 patients, of which 15% experienced stroke after infection but prior to onset of respiratory symptoms (Yaghi et al., 2020).

Precise molecular mechanisms connecting coronavirus infection and dysregulation of hemostasis are not yet clear, but several plausible explanations have been proposed, given the coordination between inflammation and hemostasis. Acute lung injury from viral cytopathic effects, the induction of the COVID-19-associated cytokine storm, complement activation, and anti-phospholipid autoantibodies have all been suggested to instigate the coagulation cascade (Merrill et al., 2020; Zuo et al., 2020).

The coagulation cascade is orchestrated by a chain reaction of serine protease zymogens that are each activated by proteolytic processing. We hypothesized that similarity in structure and sequence of trypsin-type Clan PA, Family S1A serine proteases might lead to functionally important overlap between these enzymes with regards to substrate specificity and sensitivity to inhibitors. Here, we investigate whether circulating proteases involved in blood clotting can contribute to SARS-CoV-2 spike cleavage activation and enhance viral entry.

Results

Coagulation factors directly cleave SARS-CoV-2 spike

We developed a fluorescence resonance energy transfer (FRET)-based protease enzymatic assay based on peptides containing either the S1/S2 or S2' cleavage sites of the SARS-CoV-2 S (**Fig. 1A**). Upon cleavage, the liberated 5-FAM emits fluorescent signal proportional to the quantity of product (**Fig. S1A-B**). Under fixed conditions (125nM enzyme and 10μM S1/S2 substrate), coagulation factors thrombin and factor Xa appeared to show greater activity than TMPRSS2 (**Fig. 1B**).

To determine the properties of enzyme-substrate relationships, TMPRSS2, factor Xa, and thrombin cleavage of S1/S2 and S2' peptides were determined over a range of 0-160 μM peptide substrate (**Fig. 1C-E, Table 1**). TMPRSS2-mediated S1/S2 cleavage proceeded with a higher turnover rate and higher affinity (lower K_m) than TMPRSS2-mediated S2' cleavage (**Fig. 1F-G**). Surprisingly, factor Xa catalyzed S1/S2 cleavage more than an order of magnitude faster than TMPRSS2 (**Fig. 1C-D,F**), although factor Xa showed lower affinity (higher K_m) compared with TMPRSS2 to the S1/S2 peptide (**Fig. 1C-D,G**). Thrombin has greater affinity (lower K_m) than TMPRSS2 and Factor Xa for the S1/S2 substrate (**Fig. 1G**) and performs S1/S2 cleavage at a rate intermediate between TMPRSS2 and Factor Xa (**Fig. 1F**). Unlike factor Xa, thrombin cleaves the S2' peptide with greater activity than TMPRSS2 (**Fig. 1E-H**).

Furthermore, we compared the ability of coagulation factors to cleave SARS-CoV-2 S to their ability to cleave their known substrates. During the physiological process of clotting, factor Xa cleaves prothrombin at R271, which ultimately becomes the activated form α-thrombin (Wood et al., 2011). Thrombin, in turn, cleaves fibrinogen in a critical step toward aggregation and polymerization of high molecular weight fibrin clots. Fibrinogen is composed of three polypeptide chains and the beta chain is cleaved by thrombin at R44. Fluorogenic peptides corresponding to $THRB^{R271}$ and FGB^{R44} were synthesized and assayed with TMPRSS2, factor Xa, and thrombin. TMPRSS2 exhibited relatively broad activity to cleave this collection of substrates (**Fig. 1I**). As expected, factor Xa showed strong selectivity for $THRB^{R271}$ over FGB^{R44}, while thrombin showed the opposite substrate preference (**Fig. 1J-K**). Remarkably, factor Xa showed ~9-fold greater maximum initial reaction velocity (V_{max}) in cleaving the spike S1/S2 peptide compared to cleaving its known substrate, $THRB^{R271}$ (**Fig. 1J**). The V_{max} for thrombin cleavage of the spike S1/S2 peptide was only ~4.5-fold lower than its V_{max} for the benchmark FGB^{R44} peptide (**Fig. 1K**), indicating that thrombin might also cleave this site when activated during coagulation.

We next assessed the effect of substituting amino acids adjacent to the cleavage site of the S1/S2 peptide on proteolytic cleavage by these proteases. An arginine preceding the cleavage site (P1 position) is a common feature of substrates of many serine proteases. Substitution of the P1 arginine in the S1/S2 substrate with alanine (S1S2-P1A) resulted in a 4-fold reduction in TMPRSS2 cleavage and abolished nearly all cleavage by factor Xa and thrombin (**Fig. S1C-E**). Substitutions in the P3 and P4 positions with features typical of a substrate of TTSPs (Damalanka et al., 2019) (S1S2-HPN) did not change TMPRSS2 cleavage and greatly reduced factor Xa and thrombin cleavage (**Fig. S1C-E**). Although the substrate specificity of TTSPs and coagulation factors are not uniformly similar, the sequence of the SARS-CoV-2 S1/S2 site is a substrate common to TMPRSS2, factor Xa, and thrombin.

In summary, the coagulation serine proteases factor Xa and thrombin exhibit even greater proteolytic activity against the SARS-CoV-2 peptide substrates than TMPRSS2, a protease presumed to be essential in coronavirus entry, and the S1/S2 boundary appears to be an even more optimal factor Xa substrate than peptide substrates derived from known physiological targets of factor Xa in coagulation.

Factor Xa and thrombin facilitate SARS-CoV-2 spike mediated entry

We next investigated whether coagulation factors could cleave trimeric spike in its native 3D conformation, and whether this activity potentiated spike function in viral entry into cells. To do so, we used replication-defective SARS-CoV-2 spike-pseudotyped VSV or HIV-1 virus (Schmidt et al., 2020). First, recombinant G protein-deficient vesicular stomatitis virus (rVSVΔG) was pseudotyped with SARS-CoV-2-S (**Fig. 2A**), yielding chimeric pseudovirus dependent on spike for cell entry and expression of NeonGreen and luciferase reporters (**Fig. S2A**). Addition of purified factor Xa or thrombin to the media significantly increased infection in Calu3 cells 16 hours post infection as determined by either quantification of NeonGreen (**Fig. 2B-C, S2B**) or Nanoluciferase activity (**Fig. 2D)**.

SARS-CoV-2 contains a notable insertion of basic residues at the S1/S2 boundary, distinguishing its sequence from many related betacoronaviruses (Jaimes et al., 2020b). Entry of rVSVΔG was increased when complemented with spike protein from SARS-CoV of the 2002 outbreak (**Fig. 2E**), but not when complemented instead with VSV G (**Fig. 2F**). This indicates that factor Xa spike cleavage could be relevant across multiple coronaviruses, but is not generally associated with VSV entry.

We further validated that factor Xa activated spike-mediated entry using a different pseudovirus system based on HIV-1 (**Fig. 2G-H**) (Schmidt et al., 2020). We first confirmed that HIV-1_{NL}/SARS-CoV-2 pseudovirus is dependent on ACE2 expression in target cells using A549 cells with or without ectopic ACE2 expression. While no difference is observed with VSV G-pseudotyped particles, SARS-CoV-2 pseudovirus infection is significantly higher in ACE2-expressing A549 cells (**Fig. S2C**). Caco2 cells, which endogenously express ACE2 and TMPRSS2, show greater susceptibility to SARS-CoV-2 S-pseudotyped particles, but not VSV G pseudotyped particles, when compared to A549/ACE2 cells (**Fig. S2C**).

Consistent with the results above, addition of purified Factor Xa to the media at the time of infection enhanced entry of HIV-1-based SARS-CoV-2 pseudovirus in A549/ACE2 and Vero cells. However, thrombin did not appear to enhance spike-mediated entry in this setting (**Fig. S2D-G**).

We investigated the functional interaction of TMPRSS2 expression and the effect of exogenous activated coagulation factors. A549/ACE2 and Vero cells lack endogenous TMPRSS2 expression. TMPRSS2 is expressed in Calu3 cells and contributes to coronavirus entry (Hoffmann et al., 2020a). In the HIV-1 pseudovirus system, factor Xa induced a significant dose-dependent effect on pseudovirus entry in A549/ACE2 and Calu3 cells (**Fig. 2I, J**). An

isogenic pair of Vero cells was generated by expressing TMPRSS2 or GFP. Pseudovirus infection of both $Vero^{GFP}$ and $Vero^{TMPRSS2}$ cells were significantly increased by factor Xa (**Fig. 2K**).

Finally, we generated an orthogonal functional assay of spike protein. Upon infection or ectopic expression, coronavirus spike proteins can localize to the cell membrane in mammalian cells and interact with ACE2 on neighboring cells. This can generate virion-independent cell-cell fusion *in vitro* and *in vivo* (Ou et al., 2020). By transducing and selecting 293T cells to express either ACE2/tRFP or SARS-CoV-2S/GFP, co-cultured cells would be expected to fuse heterotypically to form multinucleated syncytia (**Fig. 2L**). Overexpression of TMPRSS2 or treatment with exogenous factor Xa or thrombin resulted in significant increase in formation of double positive GFP+RFP+ cells (**Fig. 2M**). Factor Xa, and possibly thrombin, facilitate SARS-CoV-2 S-mediated entry in $ACE2^{+}TMPRSS2^{+}$ target cells and appear to expand the target cell range among $ACE2^{+}TMPRSS2^{-}$ cells.

Serine protease inhibitors suppress SARS-CoV-2 entry via inhibition of TMPRSS2

We conducted a screen of both approved and clinical trial-stage serine protease inhibitors for anti-TMPRSS2 activity using the S1/S2 FRET peptide. FDA-approved drugs that target proteases include ACE inhibitors, DPP4 inhibitors, viral protease inhibitors, and anticoagulants. Of those that target serine proteases, anticoagulants constitute the majority of approved drugs. Camostat and nafamostat resulted in strong inhibition of TMPRSS2 (**Fig. 3A**), as expected (Hoffmann et al., 2020a; Hoffmann et al., 2020c). We also identified that otamixaban and the active form of dabigatran (but not its prodrug dabigatran etexilate) inhibit TMPRSS2 enzymatic activity *in vitro* (**Fig. 3A-B**).

To confirm these results in a functional assay of spike protein, SARS-CoV-2 S-pseudotyped HIV-1 particles were employed to infect human lung Calu3 cells (**Fig. 3C**). Consistent with the TMPRSS2 enzymatic assay, camostat, nafamaostat, otamixaban, and dabigatran etexilate suppressed pseudoviral entry, as indicated by nanoluciferase luminescent signal (**Fig. 3C**). No effects on relative cell growth were observed at the same timepoint in Calu3 or A549 cells (**Fig. 3D, S3A**), confirming that reduced luminescent signal was not due to cytotoxicity. A dose-response experiment with select protease inhibitors revealed a sub-micromolar IC50 for camostat and nafamostat and IC50s in the 10-20 μM range for otamixaban and dabigatran in Calu3 cells (**Fig. 3E**). These results were further validated in the VSV pseudovirus system in multiple cell lines, where response to these candidate inhibitors was dependent on TMPRSS2 expression (**Fig. S3B-E**).

We aimed to determine whether the effects of camostat and nafamostat are indeed TMPRSS2-dependent, or if other unidentified cellular proteases can compensate for TMPRSS2 suppression. To do so, we knocked out TMPRSS2 in ACE2$^+$TMPRSS2$^+$ Caco2 cells and found that susceptibility to pseudovirus was significantly reduced, comparable to knockout of ACE2 (**Fig. 3F, S4A-J**). Furthermore, both camostat and nafamostat reduce pseudovirus entry into control Caco2 cells harboring control sgRNA targeting CD4, but this effect was abolished in cells with two independent TMPRSS2-targeting sgRNAs, (**Fig. 3G**). These data indicate that, in the absence of exogenous proteases, TMPRSS2 is the predominant enzyme activating SARS-CoV-2 spike in TMPRSS2$^+$ cells and that TMPRSS2 is likely the primary cellular target of camostat and nafamostat.

Nafamostat broadly inhibits cleavage of spike peptides by both transmembrane serine proteases and coagulation factors.

We next explored the candidate set of inhibitors for cross-reactivity against a broader set of proteases that could facilitate viral entry. Human airway trypsin-like protease (HAT), encoded by *TMPRSS11D*, exhibited sensitivity to camostat and nafamostat, similar to TMPRSS2 (**Fig. 4A-B**). Compared to TMPRSS2, HAT was more sensitive to dabigatran and less sensitive to otamixaban (**Fig. 4A-B**). Factor Xa activity against the S1/S2 peptide was most sensitive to otamixaban and moderately sensitive to nafamostat and dabigatran, while Factor Xa exhibited much less activity against S2' peptide, which was sensitive to the compounds tested (**Fig. 4C**). Thrombin activity was sensitive to camostat, nafamostat, and dabigatran, and moderately sensitive to otamixaban (**Fig. 4D**).

We performed a dose response curve of the panel of inhibitors on factor Xa and thrombin S1/S2 cleavage. Otamixaban, a designed factor Xa inhibitor, demonstrated an IC50 at the nanomolar level to factor Xa, while nafamostat and dabigatran demonstrated IC50's in the micromolar range (**Fig. 4E**). Camostat did not potently inhibit factor Xa spike cleavage. Dabigatran, a designed thrombin inhibitor, as well as nafamostat and camostat demonstrated a submicromolar IC50 for thrombin-dependent spike cleavage (**Fig. 4F**). Otamixaban inhibited thrombin spike cleavage in the micromolar range.

Furin showed high activity against the S1/S2 peptide, but not against the S2' peptide, and was not sensitive to any of the candidate inhibitors (**Fig. S5A-B**). While it has been suggested that TMPRSS4 or neutrophil elastase may also cleave SARS-CoV-2 spike, we detected minimal activity against either S1/S2 or S2' peptide substrates in our enzymatic assay (<1% of furin cleavage of S1/S2) (**Fig. S5A-B**).

Finally, nafamostat effectively suppresses SARS-CoV-2 S-mediated entry with or without the addition of exogenous factor Xa, using either the VSV-based (**Fig. 4G**) or HIV-1-based (**Fig. 4H**) SARS-CoV-2 pseudovirus. Taken together, nafamostat appears to be a versatile inhibitor of spike activation by a variety of transmembrane serine proteases (TTSPs) and coagulation factors.

Discussion

Coagulation factors cleave the SARS-CoV-2 spike protein

Using a FRET-based enzymatic assay and multiple platforms of pseudovirus and cell fusion assays, we demonstrate that factor Xa and thrombin, two serine protease coagulation factors, cleave SARS-CoV-2 spike protein. Coagulation-induced cleavage enhances spike activation and increases viral entry into target cells. Nafamostat, among currently available drugs, is best suited as a multi-purpose inhibitor against spike cleavage by TTSPs and coagulation factors. These data have numerous implications at the intersection of virology and coagulation.

Viral envelope protein activation by non-target-cell proteases

Hijacking of host transmembrane, endosomal, and ER proteases to activate viral envelope proteins has been described in influenza A, human metapneumovirus, HIV, and Sendai virus (Kido et al., 1996; Straus et al., 2020). In the present study, we find an instance where the virus is primed not by proteases expressed by the target cell, but by host organism proteases derived from the microenvironment of the target cell. Prior studies have described cleavage activation of SARS-CoV by neutrophil elastase and plasmin, illustrating that microenvironmental host proteases can indeed play an important role in coronavirus spike priming (Belouzard et al., 2010; Kam et al., 2009; Matsuyama et al., 2005). Generally, the scope by which circulating proteases, such as coagulation factors, or proteases expressed by immune cells, such as neutrophil elastase, interact with viral envelope proteins during infection has not been comprehensively explored.

Relatively few studies have examined the interaction of factor Xa or thrombin and viral proteins, and each relies on target cells as the source of coagulation factors. Our results are consistent with a prior study that concluded that factor Xa cleaves and activates SARS-CoV spike (Du et al., 2007). Traditionally, influenza vaccines rely on viral propagation in chicken eggs and factor Xa is known to be important for its proteolytic activity on hemagglutinin during this process (Gotoh et al., 1990). Hemagglutinin cleavability by Factor Xa is a potential determinant of the efficiency of strain-specific propagation of influenza A virus *in ovo* (Straus and Whittaker, 2017). Intracellularly, hepatitis E virus ORF1 polyprotein is processed by thrombin and factor Xa in the cytoplasm of host cell hepatocytes, which are the primary cell type responsible for generating and secreting coagulation factors (Kanade et al., 2018).

Activation of coagulation has the potential to exacerbate SARS-CoV-2 infectivity in both TMPRSS2+ and TMPRSS2- host cells. Reliance on extracellular proteolytic activity expands the field of susceptible cell types and regions of the airway. Extrapulmonary infection has been described, particularly in small intestinal enterocytes (Xiao et al., 2020; Zang et al., 2020) and, in some cases, the central nervous system (Song et al., 2021). It warrants investigation whether hypercoagulation is linked to extrapulmonary infection.

Evolutionary perspective on viral-host interaction.

Proteolytic cleavage of the spike forms a barrier to zoonotic crossover independent of receptor binding (Menachery et al., 2020). Hemostasis is of central importance in mammals and represents a major vulnerability of mammals to predators and pathogens, either through hyperactivation of coagulation or uncontrolled bleeding. The dysregulation of hemostasis is a convergent mechanism of toxins of snakes, bees, and bats (Ma et al., 2013; Markland and Swenson, 2013; Prado et al., 2010) and a driver of virulence in Ebola and dengue virus infection (Geisbert et al., 2003; Rathore et al., 2019). Perhaps, SARS-CoV-2 has undergone selection to both induce and exploit an environment locally enriched in coagulation proteases, instigating a positive feedback loop to promote entry into additional host cells.

Clinical relevance of potential antiviral activity of anticoagulants

Effective anticoagulation is a critical area of investigation to improve outcomes in coronavirus infection. Vitamin K antagonists, including heparin, are commonly used for preventing venous thromboembolism in COVID-19, although no strong evidence yet supports any specific anticoagulant (Cuker et al., 2021). Retrospective analysis suggested that low molecular weight heparin benefits patients with signs of coagulopathy (Tang et al., 2020). However, three large randomized clinical trials to determine the benefit of therapeutic-intensity vs. prophylactic intensity heparin in critically ill COVID-19 patients were suspended at interim analysis for futility (NCT02735707, NCT04505774, and NCT04372589); results for moderately ill hospitalized patients are pending. Optimal protocols for managing coagulopathy in COVID-19 patients have not yet been developed.

Many COVID-19 associated complications leading to hospitalization occur as immune hyperactivation waxes and peak viral titer wanes (Griffin et al., 2021). To take advantage of the potential antiviral effect of anticoagulants, early intervention in an outpatient setting would be required, where direct oral anticoagulants (DOACs) are more feasible than heparin and other

intravenously administered drugs. In consideration to drug-repurposing, we explored the utility of FDA-approved and clinical trial stage serine protease inhibitors to block SARS-CoV-2 spike cleavage. From a global health perspective, as vaccination increases and disease burden shifts to low- and middle-income countries, cost-effectiveness, stability and oral bioavailability are important considerations. It is notable that four direct oral anticoagulants, including dabigatran, have been recently added to the WHO list of essential medicines, as patents expire and prices decline (Zaidel et al., 2020). In our studies, anticoagulant serine protease inhibitors, otamixaban and dabigatran, exhibited off-target activity against TMPRSS2 and other TTSPs, but may require concentrations higher than those safely reached *in vivo* (Paccaly et al., 2006; Stangier and Clemens, 2009). Nevertheless, early intervention with DOACs have strong potential to inhibit coagulation-factor-induced SARS-CoV-2 spike cleavage as well as managing coagulopathy and thrombotic complications.

Our data suggest that nafamostat and camostat may offer three distinct therapeutic mechanisms against SARS-CoV-2 infection; these compounds have the potential to block spike cleavage mediated by TMPRSS2 and other TTSPs, to serve as an anticoagulant, and to block spike cleavage by coagulation factors. Nafamostat (Fujii and Hitomi, 1981; Keck et al., 2001; Takeda et al., 1996) and Camostat (Ramsey et al., 2019) have been in clinical use in Asia for many years for the treatment of pancreatitis. Nafamostat has also been used as an anticoagulant during hemodialysis (Akizawa et al., 1993) and extracorporeal membrane oxygenation (ECMO) (Park et al., 2015), and to manage disseminated intravascular coagulopathy (Kobayashi et al., 2001). Our results are consistent with prior experiments using a FRET-based enzymatic assay demonstrating the inhibitory activity of camostat and nafamostat against TMPRSS2 and other serine proteases using a generic peptide substrate with the sequence Asn-Ala-Arg (Shrimp et al., 2020). As of this writing, there are currently eight open clinical trials listed on clinicaltrials.gov to investigate the use of nafamostat in COVID-19, while 23 active clinical trials of camostat for COVID-19 were identified. Inhibition of coagulation factor-induced spike cleavage may contribute to the molecular mechanism of these agents, if treatment is given sufficiently early.

The most prominent risk of anticoagulants is bleeding, and notably direct oral anticoagulants have a reduced risk of intracranial hemorrhage and other bleeding events compared to vitamin K antagonists (Chen et al., 2020; Hellenbart et al., 2017). Also, nafamostat has less bleeding risk than heparin (Makino et al., 2016). Coagulation is a host defense system that is intimately linked to immunity. Clotting factors can activate the PAR-IFNβ pathway,

modulating the innate immune response during viral infection (Antoniak et al., 2013; Antoniak et al., 2017). Anticoagulation has been observed to either limit or promote lung injury, depending on the model of infection (Choi et al., 2008; Tatsumi et al., 2016).

Limitations

The experiments of this study, like prior studies using similar techniques, have some limitations. Protease enzymatic assays on peptide substrates allow for detailed biochemical characterization of a specific site, but peptide substrates may not have the equivalent three-dimensional conformation or post-translational modifications of the full-length protein produced in appropriate cells. For instance, SARS-CoV-2 S is extensively glycosylated (Watanabe et al., 2020). Pseudovirus and syncytia formation provide complementary functional assays, dependent on homotrimeric spike protein produced in human cells. The possibility of additional spike cleavage sites and potential pro- and anti-viral consequence of proteases acting on cell surface proteins including ACE2 cannot be excluded. The amount, density, and accessibility of spike protein could be different between these cell-based surrogate assays and wild type SARS-CoV-2 infection. However, antibody neutralization is highly correlated between authentic virus and corresponding pseudotyped viruses, suggesting similar conformation (Schmidt et al., 2020). We have mitigated the risk of artifact by using multiple orthogonal platforms, including VSV-based pseudovirus, HIV-based pseudovirus, and syncytia formation.

Conclusion

Collectively, our data provide rationale for the investigation of early intervention with judiciously selected anticoagulant treatment, which may have collateral benefit in limiting progressive spread of SARS-CoV-2 infection throughout the lung in infected individuals. Preparedness to mitigate a future SARS-CoV-3 epidemic is critical to pursue through the understanding of coronavirus-host interactions.

Author Contributions

Conceptualization, E.R.K and L.C.C.; Methodology, E.R.K, J.A.J., J.L.J., F.M., Y.W.; Investigation, E.R.K., J.A.J., M.M, A.E.S., Y.B.; Writing – Original Draft, E.R.K. and L.C.C.; Writing – Review & Editing, E.R.K., J.L.J., F.M., Y.B., R.E.S., G.W., and L.C.C.; Funding Acquisition, R.E.S., G.W., and L.C.C.; Resources, F.M., Y.W.; Supervision, R.E.S., G.W., and L.C.C..

Acknowledgements

The authors would like to thank Pilar Mendoza (Rockefeller University), John Blenis, Elena Piskounova, Tim McGraw, Benjamin Turk, Marco Straus, Tomer Yaron, and all members of the Cantley Lab for insightful discussion and helpful comments. We thank Paul Bieniasz (Rockefeller University) and Theodora Hatziioannou (Rockefeller University) for providing reagents and helping to establish the pseudovirus platform in our laboratory. We thank Danielle Bulaon (Weill Cornell) for provisioning inhibitors, Benjamin tenOever (Mount Sinai) for providing Vero cells, and Francisco Sanchez-Rivera and Scott Lowe (MSKCC) for the ipUSEPR plasmid. This work was funded in part by the National Institute of Health research grant R01AI35270 (to GW).

Declarations of Interests

LCC is a founder and member of the SAB of Agios Pharmaceuticals and a founder and former member of the SAB of Ravenna Pharmaceuticals (previously Petra Pharmaceuticals). These companies are developing novel therapies for cancer. LCC holds equity in Agios. LCC's laboratory also received some financial support from Ravenna Pharmaceuticals. RES is on the scientific advisory board for Miromatrix Inc and is a consultant and speaker for Alnylam Inc.

Figure Legends

Figure 1. Coagulation factors directly cleave SARS-CoV-2 spike. (**A**) Peptides derived from two known cleavage sites of SARS-CoV-2 spike were designed with C-terminal fluorophore 5-FAM and N-terminal FRET quencher QXL-520. (**B**) Cleavage of 10 μM S1/S2 peptide substrate incubated with 125nM TMPRSS2, factor Xa, or thrombin. Initial velocities for the cleavage of SARS-CoV-2 spike S1/S2 and S2' peptide substrates by (**C**) TMPRSS2, (**D**) Factor Xa, and (**E**) Thrombin were measured over a range of 0-160 μM substrate. From initial velocity values, enzyme kinetic constants (**F**) turnover rate K_{cat} (s^{-1}), (**G**) affinity constant K_m, and (**H**) specificity constant (K_{cat}/K_m) were obtained for the indicated enzymes with S1/S2 and S2' peptides. (**I-K**) Heatmaps depict the initial velocity V_0 of cleavage of the indicated peptide substrates and concentrations by (**I**) TMPRSS2, (**J**) factor Xa, and (**K**) thrombin.

Figure 2. **Factor Xa and thrombin facilitate SARS-CoV-2 spike mediated entry.** (**A**) Schematic of constructs used to generate SARS-CoV-2 spike-pseudotyped/VSV-based particles. (**B**) Timeline of VSV-based pseudovirus experiments. (**C**) Calu3 cells were infected with rVSVΔG/SARS-CoV-2 pseudovirus with concomitant treatment with vehicle, 250nM factor Xa, or 250nM thrombin. Quantification of the ratio of green fluorescent area to total confluence. (4 fields/replicate well, 4 wells/condition). (**D**) Nanoluciferase luminescent signal was measured following infection with rVSVΔG/SARS-CoV-2 pseudovirus and the addition of either vehicle, factor Xa, or thrombin. The effect of factor Xa on rVSVΔG complemented with either (**E**) SARS-CoV spike or (**F**) VSV-G was measured by luminescent signal. (**G**) Schematic of constructs used to generate SARS-CoV-2 spike-pseudotyped/HIV-1-based particles. (**H**) Timeline of HIV-1-based pseudovirus experiments. Luminescent signal was measured following HIV-1_{NL}/SARS-CoV-2 pseudovirus infection and concomitant treatment with 125-250nM factor Xa in (**I**) A549/ACE2 and (**J**) Calu3 cells. (**K**) Vero cells were transduced with lentiviral vectors to express GFP or TMPRSS2. Following selection, cells were infected with HIV-1_{NL}/SARS-CoV-2 pseudovirus and concomitantly treated with 125-250nM factor Xa. Subsequently, Nanoluciferase luminescent signal was determined and plotted relative to vehicle-treated control. (**L**) By transducing and selecting 293T cells to express either ACE2/tRFP or SARS-CoV-2S/GFP, co-cultured cells fuse heterotypically to form multinucleated syncytia (**M**) Number of fused GFP+RFP+ cells were quantified by flow cytometry 24 hours after co-culture of ACE2- and spike-expressing cells. * $P<0.05$, two-tailed t-test. Error bars represent +/- SEM.

Figure 3. Anticoagulant serine protease inhibitors suppress SARS-CoV-2 entry via inhibition of TMPRSS2. (**A**) FDA-approved and investigational serine protease inhibitors were screened by enzymatic assay to inhibit TMPRSS2 cleavage of SARS-CoV-2 S1/S2 peptide substrate. Relative change in fluorescence with respect to DMSO vehicle is shown. Colors indicate the described target of the drugs screened. All drugs screened at 10 μM final concentration. (**B**) Active form of dabigatran in enzymatic assay for TMPRSS2 inhibition. Relative fluorescence with respect to 0.1N HCl vehicle is shown. (**C**) Calu3 cells were treated with 10 μM of the indicated drugs for 24 hr prior to infection with HIV-1_{NL}/SARS-CoV-2 pseudovirus. Media was changed at 24 hr post infection and pseudoviral entry was measured by Nanoluciferase luminescent signal at 40 hr. (**D**) Calu3 cells treated with 10 μM of the indicated drugs were monitored for confluence by Incucyte for 40 hr. (**E**) Pseudoviral entry was measured by Nanoluciferase luminescent signal in Calu3 cells treated various concentrations of the indicated drugs for 4 hours prior to infection with SARS-CoV-2 pseudovirus. (**F**) Caco2 cells were infected with lenti-Cas9-blast and U6-sgRNA-EFS-puro-P2A-tRFP and selected. Neutral controls targeting CD4 (not endogenously expressed) or PHGDH intron 1, two sgRNAs each targeting different regions of ACE2 and TMPRSS2 were included. Cells were subsequently infected with HIV-1_{NL}/SARS-CoV-2 pseudovirus. (**G**) Caco2 cells co-expressing Cas9 and sgRNAs targeting CD4 (not expressed) or TMPRSS2 were treated with 10μM Camostat, Nafamostat, or DMSO vehicle. * $P<0.05$, two-tailed t-test. Error bars +/- SEM.

Figure 4. Nafamostat broadly inhibits cleavage of spike peptides by both coagulation factors and transmembrane serine proteases. Initial velocities for the cleavage of 10 μM SARS-CoV-2 spike S1/S2 (top) and S2' (bottom) peptide substrates by (**A**) TMPRSS2, (**B**) TMPRSS11D/Human airway trypsin-like protease (**C**) factor Xa, and (**D**) thrombin were measured in the presence of DMSO vehicle, or 10μM camostat, nafamostat, otamixaban, or dabigatran. The relative activity of (**E**) factor Xa and (**F**) thrombin were determined over a range of 0-10μM of the indicated drugs. Calu3 cells were treated with a range of concentrations of nafamostat with or without addition of 250 nM exogenous factor Xa and infected with (**G**) rVSVΔG/SARS-CoV-2 pseudovirus or (**H**) HIV-1_{NL}/SARS-CoV-2 pseudovirus and infectivify was measured by luminescence. Error bars +/- SEM.

Table 1. Kinetics of SARS-CoV-2 spike peptide substrate cleavage. Kinetic constants obtained from initial velocity studies with varying concentrations of SARS-CoV-2 spike S1/S2 and S2' peptide substrates. Each estimate is based on seven different concentrations of substrate in 1:2 serial dilution (0-160 μM).

Supplementary Data

Supplementary Figure 1. Optimization of FRET enzymatic assay, related to Figure 1. (**A**) TMPRSS2 enzymatic assay was performed in AB1 (20mM Tris-HCl, pH7.3, 100 mM NaCl, 1 mM EDTA, fresh 1 mM DTT) or AB2 (50mM Tris-HCl, 150mM NaCl, pH 8) using 10 μM of either S1/S2 or S2' peptide substrate. (**B**) Titration of enzyme concentration was performed (0-1000 nM) with 10 μM S1/S2 substrate. Initial reaction velocity V_0 (rate of change in fluorescent signal) each enzyme concentration with 10μM S1/S2 peptide substrate. (**C-E**) Initial reaction velocity with respect to enzyme concentration for peptide substrates of the SARS-CoV-2 spike S1/S2 site (S1S2), with P1 arginine substituted with alanine (S1S2-P1A), or with substitutions in the P3 and P4 position (RR>SQ) with (**C**) TMPRSS2, (**D**) factor Xa, or (**E**) thrombin. (**F**) List of peptide substrates used in this study.

Supplementary Figure 2. Further characterization of SARS-CoV-2 pseudovirus, related to Figure 2. (**A**) Nanoluciferase luminescent signal following addition of rVSVΔG pseudovirus complemented with VSV G, SARS-CoV-2 S, SARS-CoV S, or without complementation with any envelope protein to Calu3 cells. Each pseudovirus was titrated by adding the indicated volume of inoculum, supplemented with fresh media up to 200 ul/well in a 96W plate. (**B**) Representative merged brightfield and green fluorescence images of Calu3 cells without infection or following rVSVΔG/SARS-CoV-2 pseudovirus infection and concomitant treatment with vehicle, 250nM factor Xa, or 250nM thrombin (corresponding to **Fig. 2C**). Scale bars represent 300 μm. (**C**) A549 cells (which do not express ACE2), A549/ACE2 cells (ectopic ACE2 expression from a lentiviral vector), and Caco2 cells (which express endogenous ACE2 and TMPRSS2) infected with HIV-1_{NL}-based particles pseudotyped with SARS-CoV-2 S or VSV G. (**D-G**) HIV-1_{NL}/SARS-CoV-2 pseudovirus with addition of purified protease or vehicle. Nanoluciferase luminescent signal relative to vehicle-treated control was measured following infection in (**D**) A549/ACE2 and (**E**) Vero cells. Cell number following protease treatment, relative to vehicle control was determined for (**F**) A549/ACE2 and (**G**) Vero cells. * $P<0.05$, two-tailed t-test. Error bars +/- SEM.

Supplementary Figure 3. **Further characterization of antiviral activity of serine protease inhibitors, related to Figure 3.** (**A**) Confluence of A549 cell following 48 hours of treatment with 10μM protease inhibitors, normalized to DMSO vehicle control. (**B-E**) Nanoluciferase luminescent signal following infection of (**B**) Caco2 (**C**) Calu3, (**D**) A549/ACE2, or (**E**) Vero cells with HIV-1_{NL}/SARS-CoV-2 pseudovirus pretreated for 4 hours with 10 μM camostat, nafamostat, dabigatran, or otamixaban, compared with uninfected or infected/untreated cells. Expression status of ACE2 and TMPRSS2 for each cell line is indicated.

Supplementary Figure 4. **Evidence of CRISPR knockout efficiency, related to Figure 3.** (**A**) Constructs used for CRISPR experiments. (**B**) Percentage of reads exhibiting wild type, frameshift, or in-frame indels at each locus for the indicated sgRNAs. (**C-E**) Distribution of reads with deletion or insertion by position within amplicon. (**G-J**) Distribution of the size of insertions and deletions in each amplicon. Two sgRNAs targeting ACE2 (g1 and g2) and two sgRNAs targeting TMPRSS2 (g1 and g2) were analyzed.

Supplementary Figure 5. Activity of candidate inhibitors against other proteases, related to Figure 4. Initial reaction velocity V_0 of furin, TMPRSS4, or neutrophil elastase cleavage of (**A**) S1/S2 peptide substrate or (**B**) S2' peptide substrate, treated with DMSO vehicle, camostat, nafamostat, otamixaban, or dabigatran. 10μM Substrate and 10μM inhibitor were used.

Methods

Enzymatic Assay

Thrombin (605195) and Factor Xa, activated by Russell's Viper Venom, were obtained from Millipore Sigma (69036). TMPRSS2, purified from yeast, was obtained from LSBio (LS-G57269). TMPRSS4 was obtained from Aviva System Biology (OPCA0240), furin was obtained from Thermo Fisher Scientific (1503SE010), neutrophil elastase was obtained from Thermo Fisher Scientific (9167SE020), Cathepsin L was obtained from Thermo Fisher Scientific (952CY010). FRET peptides were obtained from Anaspec and a peptide sequences are listed in **Supplementary Fig S1F**. Protease assay buffer was composed of 50mM Tris-HCl, 150mM NaCl, pH 8. Enzyme dilution/storage buffer was 20mM Tris-HCl, 500mM NaCl, 2mM $CaCl_2$, 50% glycerol, pH 8. Peptides were reconstituted and diluted in DMSO. Enzyme kinetics were assayed in black 96W plates with clear bottom and measured using a BMG Labtech FLUOstar Omega plate reader, reading fluorescence (excitation 485nm, emission 520nm) every minute for 20 cycles, followed by every 5 minutes for an additional 8 cycles. A standard curve of 5-FAM from 0-10 μM (1:2 serial dilutions) was used to convert RFU to μM of cleaved FRET peptide product. Calculation of enzyme constants was performed with Graphpad Prism software (version 9.0). Camostat and nafamostat were obtained from Selleck Chemicals and all other inhibitors were obtained from MedChem Express.

Cell Culture

Calu3, A549, Caco2, and Vero cells were tested for mycoplasma (Lonza MycoAlert detection kit) and human cell line identity was authenticated by ATCC. A549 and Vero cells were grown in DMEM, supplemented with 10% FBS, 100U/ml Penicillin, and 100ug/ml Streptomycin. Calu3 and Caco2 cells were grown in MEM, supplemented with 10% FBS, 100U/ml Penicillin, 100ug/ml Streptomycin, 1% MEM NEAA and 1mM sodium pyruvate.

Plasmids and lentivirus infection

Overexpression constructs pEGPN-GFP, pEGPN-ACE2, and pEGPN-TMPRSS2 were constructed by Gibson cloning using NEBuilder master mix (New England Biolabs, E2621) with overlapping PCR generated inserts for promoter EF1α, the gene of interest, promoter PGK, and neomycin/resistance gene. Lentiviral vectors were co-transduced with MD2G and PAX2 in 293T cells (5 million cells/10cm plate) with 25ul of XtremeGene9 (Millipore Sigma, #6365787001) and supernatant was harvested at 48hr and 72hr post transfection. Target cells were transduced

with the addition of 4 μg/ml polybrene (Santa Cruz, sc-134220). Infected cells were selected and maintained in 500 ug/ml G418 (Life Technologies, #10131027). lentiCas9-Blast was a gift from Feng Zhang (Sanjana et al., 2014) (Addgene plasmid # 52962). ipUSEPR was a gift from Francisco Sanchez-Rivera and Scott Lowe. sgRNAs were selected from the Brunello CRISPR database (Doench et al., 2016). Four guides per gene were tested in Caco2 cells and the most efficient two sgRNAs/gene were used in subsequent experiments (**Supplementary Fig. S4**). Knockout efficiency was determined by next-generation amplicon sequencing.

Pseudovirus

Recombinant VSV-based and HIV-1-based SARS-CoV-2 pseudovirus was generated as described previously (Schmidt et al., 2020). To generate rVSVΔG/SARS-CoV-2 pseudovirus, 293T cells (12 million cells/15cm plate) were transfected with 12.5 μg pSARS-CoV-$2_{\Delta 19}$, and 24 hr post-transfection, were infected with VSV-G-complemented rVSVΔG virus at an MOI of 1. Supernatant was collected 16 hr post-infection, centrifuged at 350 g x 10min, filtered through a 0.45-μm filter, and concentrated using Lenti-X-Concentrator (Takara Bio). Prior to infection of target cells, the viral stock was incubated with anti-VSV-G antibody (3ug/ml) for 1 h at 37°C to neutralize contaminating rVSVΔG/NG/NanoLuc/VSV-G particles.

To generate HIV-1_{NL}/SARS-CoV-2 pseudovirus, 293T cells (12 million cells/15cm plate) were co-transfected with 15.75 μg CCNanoLuc/GFP, 15.75 μg HIV-1_{NL} GagPol, and 5.625 μg CMV-SARS-CoV-2-S, using 50ul per 15cm plate X-tremeGENE 9 (Sigma-Aldrich, 8724121001). Media was changed at 24 hr post-transfection, and supernatant was collected at 48 hr and 72 hr. Centrifuged and filtered pseudovirus was concentrated with Lenti-X-concentrator or with 40% (w/v) PEG-8000, 1.2 M NaCl, pH 7.2.

Syncytia assay

293T cells were infected with lentiviral vector pEGPPR-ACE2 and selected with puromycin or infected with lentiviral vector pRRL-Spike-PBG and selected with blasticidin. ACE2- and Spike-expressing cells were mixed at a 1:1 ratio for a total of 60,000 cells per well in 96W plates. Exogenous proteases were added at the time of cell plating. GFP+RFP+ cells were quantified using a BD Attune NxT Flow cytometer (Thermo Fisher Scientific) and data was analyzed in FlowJo version 10.7.1.

Incucyte

Cells were imaged and analyzed using an Incucyte ZOOM (Essen BioScience). Four fields of view per well were averaged and 3-6 wells/condition were assayed in each experiment. Confluence was calculated from bright field images, GFP/Neon Green object confluence was calculated from green fluorescent images taken with 400ms exposure time, and GFP+ fractional area is the ratio of these variables.

Luciferase assay

Following pseudovirus infection, cells were washed twice with PBS, which was subsequently aspirated. Lysis buffer (Promega, E1531) was added (50μl/well) and incubated rotating for 15 min at room temperature. NanoGlo Substrate (Promega, N1130) was diluted 1:50 in assay buffer and 25μl/well was added and incubated for an additional 15 min. Samples were transferred to a white, opaque-bottom 96W plate and luminescence was read using a BMG Labtech FLUOstar Omega plate reader.

References:

Akizawa, T., Koshikawa, S., Ota, K., Kazama, M., Mimura, N., and Hirasawa, Y. (1993). Nafamostat mesilate: a regional anticoagulant for hemodialysis in patients at high risk for bleeding. Nephron *64*, 376-381. 10.1159/000187357

Amanat, F., Strohmeier, S., Rathnasinghe, R., Schotsaert, M., Coughlan, L., Garcia-Sastre, A., and Krammer, F. (2021). Introduction of Two Prolines and Removal of the Polybasic Cleavage Site Lead to Higher Efficacy of a Recombinant Spike-Based SARS-CoV-2 Vaccine in the Mouse Model. mBio *12*. 10.1128/mBio.02648-20

Antoniak, S., Owens, A.P., 3rd, Baunacke, M., Williams, J.C., Lee, R.D., Weithauser, A., Sheridan, P.A., Malz, R., Luyendyk, J.P., Esserman, D.A.*, et al.* (2013). PAR-1 contributes to the innate immune response during viral infection. J Clin Invest *123*, 1310-1322. 10.1172/JCI66125

Antoniak, S., Tatsumi, K., Bode, M., Vanja, S., Williams, J.C., and Mackman, N. (2017). Protease-Activated Receptor 1 Enhances Poly I:C Induction of the Antiviral Response in Macrophages and Mice. J Innate Immun *9*, 181-192. 10.1159/000450853

Baden, L.R., El Sahly, H.M., Essink, B., Kotloff, K., Frey, S., Novak, R., Diemert, D., Spector, S.A., Rouphael, N., Creech, C.B.*, et al.* (2020). Efficacy and Safety of the mRNA-1273 SARS-CoV-2 Vaccine. N Engl J Med. 10.1056/NEJMoa2035389

Belouzard, S., Chu, V.C., and Whittaker, G.R. (2009). Activation of the SARS coronavirus spike protein via sequential proteolytic cleavage at two distinct sites. Proc Natl Acad Sci U S A *106*, 5871-5876. 10.1073/pnas.0809524106

Belouzard, S., Madu, I., and Whittaker, G.R. (2010). Elastase-mediated activation of the severe acute respiratory syndrome coronavirus spike protein at discrete sites within the S2 domain. J Biol Chem *285*, 22758-22763. 10.1074/jbc.M110.103275

Benton, D.J., Wrobel, A.G., Xu, P., Roustan, C., Martin, S.R., Rosenthal, P.B., Skehel, J.J., and Gamblin, S.J. (2020). Receptor binding and priming of the spike protein of SARS-CoV-2 for membrane fusion. Nature *588*, 327-330. 10.1038/s41586-020-2772-0

Berger, I., and Schaffitzel, C. (2020). The SARS-CoV-2 spike protein: balancing stability and infectivity. Cell Res *30*, 1059-1060. 10.1038/s41422-020-00430-4

Bertram, S., Dijkman, R., Habjan, M., Heurich, A., Gierer, S., Glowacka, I., Welsch, K., Winkler, M., Schneider, H., Hofmann-Winkler, H.*, et al.* (2013). TMPRSS2 activates the human coronavirus 229E for cathepsin-independent host cell entry and is expressed in viral target cells in the respiratory epithelium. J Virol *87*, 6150-6160. 10.1128/JVI.03372-12

Bestle, D., Heindl, M.R., Limburg, H., Van Lam van, T., Pilgram, O., Moulton, H., Stein, D.A., Hardes, K., Eickmann, M., Dolnik, O.*, et al.* (2020). TMPRSS2 and furin are both essential for proteolytic activation of SARS-CoV-2 in human airway cells. Life Sci Alliance *3*. 10.26508/lsa.202000786

Bosch, B.J., Bartelink, W., and Rottier, P.J. (2008). Cathepsin L functionally cleaves the severe acute respiratory syndrome coronavirus class I fusion protein upstream of rather than adjacent to the fusion peptide. J Virol *82*, 8887-8890. 10.1128/JVI.00415-08

Chen, A., Stecker, E., and B, A.W. (2020). Direct Oral Anticoagulant Use: A Practical Guide to Common Clinical Challenges. J Am Heart Assoc *9*, e017559. 10.1161/JAHA.120.017559

Cheng, V.C., Lau, S.K., Woo, P.C., and Yuen, K.Y. (2007). Severe acute respiratory syndrome coronavirus as an agent of emerging and reemerging infection. Clin Microbiol Rev *20*, 660-694. 10.1128/CMR.00023-07

Choi, G., Hofstra, J.J., Roelofs, J.J., Rijneveld, A.W., Bresser, P., van der Zee, J.S., Florquin, S., van der Poll, T., Levi, M., and Schultz, M.J. (2008). Antithrombin inhibits bronchoalveolar activation of coagulation and limits lung injury during Streptococcus pneumoniae pneumonia in rats. Crit Care Med *36*, 204-210. 10.1097/01.CCM.0000292012.87482.F4

Consortium, W.H.O.S.T., Pan, H., Peto, R., Henao-Restrepo, A.M., Preziosi, M.P., Sathiyamoorthy, V., Abdool Karim, Q., Alejandria, M.M., Hernandez Garcia, C., Kieny, M.P.*, et al.* (2020). Repurposed Antiviral Drugs for Covid-19 - Interim WHO Solidarity Trial Results. N Engl J Med. 10.1056/NEJMoa2023184

Cuker, A., Tseng, E.K., Nieuwlaat, R., Angchaisuksiri, P., Blair, C., Dane, K., Davila, J., DeSancho, M.T., Diuguid, D., Griffin, D.O.*, et al.* (2021). American Society of Hematology 2021 guidelines on the use of anticoagulation for thromboprophylaxis in patients with COVID-19. Blood Adv *5*, 872-888. 10.1182/bloodadvances.2020003763

Damalanka, V.C., Han, Z., Karmakar, P., O'Donoghue, A.J., La Greca, F., Kim, T., Pant, S.M., Helander, J., Klefstrom, J., Craik, C.S.*, et al.* (2019). Discovery of Selective Matriptase and Hepsin Serine Protease Inhibitors: Useful Chemical Tools for Cancer Cell Biology. J Med Chem *62*, 480-490. 10.1021/acs.jmedchem.8b01536

Doench, J.G., Fusi, N., Sullender, M., Hegde, M., Vaimberg, E.W., Donovan, K.F., Smith, I., Tothova, Z., Wilen, C., Orchard, R.*, et al.* (2016). Optimized sgRNA design to maximize activity and minimize off-target effects of CRISPR-Cas9. Nat Biotechnol *34*, 184-191. 10.1038/nbt.3437

Du, L., Kao, R.Y., Zhou, Y., He, Y., Zhao, G., Wong, C., Jiang, S., Yuen, K.Y., Jin, D.Y., and Zheng, B.J. (2007). Cleavage of spike protein of SARS coronavirus by protease

factor Xa is associated with viral infectivity. Biochem Biophys Res Commun *359*, 174-179. 10.1016/j.bbrc.2007.05.092

Fujii, S., and Hitomi, Y. (1981). New synthetic inhibitors of C1r, C1 esterase, thrombin, plasmin, kallikrein and trypsin. Biochim Biophys Acta *661*, 342-345. 10.1016/0005-2744(81)90023-1

Ge, X.Y., Li, J.L., Yang, X.L., Chmura, A.A., Zhu, G., Epstein, J.H., Mazet, J.K., Hu, B., Zhang, W., Peng, C.*, et al.* (2013). Isolation and characterization of a bat SARS-like coronavirus that uses the ACE2 receptor. Nature *503*, 535-538. 10.1038/nature12711

Geisbert, T.W., Young, H.A., Jahrling, P.B., Davis, K.J., Kagan, E., and Hensley, L.E. (2003). Mechanisms underlying coagulation abnormalities in ebola hemorrhagic fever: overexpression of tissue factor in primate monocytes/macrophages is a key event. J Infect Dis *188*, 1618-1629. 10.1086/379724

Glowacka, I., Bertram, S., Muller, M.A., Allen, P., Soilleux, E., Pfefferle, S., Steffen, I., Tsegaye, T.S., He, Y., Gnirss, K.*, et al.* (2011). Evidence that TMPRSS2 activates the severe acute respiratory syndrome coronavirus spike protein for membrane fusion and reduces viral control by the humoral immune response. J Virol *85*, 4122-4134. 10.1128/JVI.02232-10

Gotoh, B., Ogasawara, T., Toyoda, T., Inocencio, N.M., Hamaguchi, M., and Nagai, Y. (1990). An endoprotease homologous to the blood clotting factor X as a determinant of viral tropism in chick embryo. EMBO J *9*, 4189-4195.

Griffin, D.O., Brennan-Rieder, D., Ngo, B., Kory, P., Confalonieri, M., Shapiro, L., Iglesias, J., Dube, M., Nanda, N., In, G.K.*, et al.* (2021). The Importance of Understanding the Stages of COVID-19 in Treatment and Trials. AIDS Rev. 10.24875/AIDSRev.200001261

Hellenbart, E.L., Faulkenberg, K.D., and Finks, S.W. (2017). Evaluation of bleeding in patients receiving direct oral anticoagulants. Vasc Health Risk Manag *13*, 325-342. 10.2147/VHRM.S121661

Hoffmann, M., Kleine-Weber, H., Schroeder, S., Kruger, N., Herrler, T., Erichsen, S., Schiergens, T.S., Herrler, G., Wu, N.H., Nitsche, A.*, et al.* (2020a). SARS-CoV-2 Cell Entry Depends on ACE2 and TMPRSS2 and Is Blocked by a Clinically Proven Protease Inhibitor. Cell *181*, 271-280 e278. 10.1016/j.cell.2020.02.052

Hoffmann, M., Mosbauer, K., Hofmann-Winkler, H., Kaul, A., Kleine-Weber, H., Kruger, N., Gassen, N.C., Muller, M.A., Drosten, C., and Pohlmann, S. (2020b). Chloroquine does not inhibit infection of human lung cells with SARS-CoV-2. Nature *585*, 588-590. 10.1038/s41586-020-2575-3

Hoffmann, M., Schroeder, S., Kleine-Weber, H., Muller, M.A., Drosten, C., and Pohlmann, S. (2020c). Nafamostat Mesylate Blocks Activation of SARS-CoV-2: New Treatment Option for COVID-19. Antimicrob Agents Chemother *64*. 10.1128/AAC.00754-20

Huang, C., Wang, Y., Li, X., Ren, L., Zhao, J., Hu, Y., Zhang, L., Fan, G., Xu, J., Gu, X.*, et al.* (2020). Clinical features of patients infected with 2019 novel coronavirus in Wuhan, China. Lancet *395*, 497-506. 10.1016/S0140-6736(20)30183-5

Hwang, D.M., Chamberlain, D.W., Poutanen, S.M., Low, D.E., Asa, S.L., and Butany, J. (2005). Pulmonary pathology of severe acute respiratory syndrome in Toronto. Mod Pathol *18*, 1-10. 10.1038/modpathol.3800247

Iwata-Yoshikawa, N., Okamura, T., Shimizu, Y., Hasegawa, H., Takeda, M., and Nagata, N. (2019). TMPRSS2 Contributes to Virus Spread and Immunopathology in the Airways of Murine Models after Coronavirus Infection. J Virol *93*. 10.1128/JVI.01815-18

Jaimes, J., Millet, J., and Whittaker, G. (2020a). Proteolytic Cleavage of the SARS-CoV-2 Spike Protein and the Role of the Novel S1/S2 Site. SSRN, 3581359. 10.2139/ssrn.3581359

Jaimes, J.A., Andre, N.M., Chappie, J.S., Millet, J.K., and Whittaker, G.R. (2020b). Phylogenetic Analysis and Structural Modeling of SARS-CoV-2 Spike Protein Reveals an Evolutionary Distinct and Proteolytically Sensitive Activation Loop. J Mol Biol *432*, 3309-3325. 10.1016/j.jmb.2020.04.009

Jaimes, J.A., Millet, J.K., Goldstein, M.E., Whittaker, G.R., and Straus, M.R. (2019). A Fluorogenic Peptide Cleavage Assay to Screen for Proteolytic Activity: Applications for coronavirus spike protein activation. J Vis Exp. 10.3791/58892

Jaimes, J.A., Millet, J.K., and Whittaker, G.R. (2020c). Proteolytic Cleavage of the SARS-CoV-2 Spike Protein and the Role of the Novel S1/S2 Site. iScience *23*, 101212. 10.1016/j.isci.2020.101212

Johnson, B.A., Xie, X., Bailey, A.L., Kalveram, B., Lokugamage, K.G., Muruato, A., Zou, J., Zhang, X., Juelich, T., Smith, J.K.*, et al.* (2021). Loss of furin cleavage site attenuates SARS-CoV-2 pathogenesis. Nature. 10.1038/s41586-021-03237-4

Kam, Y.W., Okumura, Y., Kido, H., Ng, L.F., Bruzzone, R., and Altmeyer, R. (2009). Cleavage of the SARS coronavirus spike glycoprotein by airway proteases enhances virus entry into human bronchial epithelial cells in vitro. PLoS One *4*, e7870. 10.1371/journal.pone.0007870

Kanade, G.D., Pingale, K.D., and Karpe, Y.A. (2018). Activities of Thrombin and Factor Xa Are Essential for Replication of Hepatitis E Virus and Are Possibly Implicated in ORF1 Polyprotein Processing. J Virol *92*. 10.1128/JVI.01853-17

Keck, T., Balcom, J.H., Antoniu, B.A., Lewandrowski, K., Warshaw, A.L., and Fernandez-del Castillo, C.F. (2001). Regional effects of nafamostat, a novel potent protease and complement inhibitor, on severe necrotizing pancreatitis. Surgery *130*, 175-181. 10.1067/msy.2001.115827

Kido, H., Niwa, Y., Beppu, Y., and Towatari, T. (1996). Cellular proteases involved in the pathogenicity of enveloped animal viruses, human immunodeficiency virus, influenza virus A and Sendai virus. Adv Enzyme Regul *36*, 325-347. 10.1016/0065-2571(95)00016-x

Kipshidze, N., Dangas, G., White, C.J., Kipshidze, N., Siddiqui, F., Lattimer, C.R., Carter, C.A., and Fareed, J. (2020). Viral Coagulopathy in Patients With COVID-19: Treatment and Care. Clin Appl Thromb Hemost *26*, 1076029620936776. 10.1177/1076029620936776

Kleine-Weber, H., Elzayat, M.T., Hoffmann, M., and Pohlmann, S. (2018). Functional analysis of potential cleavage sites in the MERS-coronavirus spike protein. Sci Rep *8*, 16597. 10.1038/s41598-018-34859-w

Kobayashi, T., Terao, T., Maki, M., and Ikenoue, T. (2001). Diagnosis and management of acute obstetrical DIC. Semin Thromb Hemost *27*, 161-167. 10.1055/s-2001-14076

Kwok, K.O., Li, K.K., Wei, W.I., Tang, A., Wong, S.Y.S., and Lee, S.S. (2020). Influenza vaccine uptake, COVID-19 vaccination intention and vaccine hesitancy among nurses: A survey. Int J Nurs Stud *114*, 103854. 10.1016/j.ijnurstu.2020.103854

Lin, C., Tu, P., and Beitsch, L.M. (2020). Confidence and Receptivity for COVID-19 Vaccines: A Rapid Systematic Review. Vaccines (Basel) *9*. 10.3390/vaccines9010016

Ma, D., Mizurini, D.M., Assumpcao, T.C., Li, Y., Qi, Y., Kotsyfakis, M., Ribeiro, J.M., Monteiro, R.Q., and Francischetti, I.M. (2013). Desmolaris, a novel factor XIa anticoagulant from the salivary gland of the vampire bat (Desmodus rotundus) inhibits inflammation and thrombosis in vivo. Blood *122*, 4094-4106. 10.1182/blood-2013-08-517474

Makino, S., Egi, M., Kita, H., Miyatake, Y., Kubota, K., and Mizobuchi, S. (2016). Comparison of nafamostat mesilate and unfractionated heparin as anticoagulants during continuous renal replacement therapy. Int J Artif Organs *39*, 16-21. 10.5301/ijao.5000465

Markland, F.S., Jr., and Swenson, S. (2013). Snake venom metalloproteinases. Toxicon *62*, 3-18. 10.1016/j.toxicon.2012.09.004

Matsuyama, S., Ujike, M., Morikawa, S., Tashiro, M., and Taguchi, F. (2005). Protease-mediated enhancement of severe acute respiratory syndrome coronavirus infection. Proc Natl Acad Sci U S A *102*, 12543-12547. 10.1073/pnas.0503203102

McGonagle, D., O'Donnell, J.S., Sharif, K., Emery, P., and Bridgewood, C. (2020). Immune mechanisms of pulmonary intravascular coagulopathy in COVID-19 pneumonia. Lancet Rheumatol *2*, e437-e445. 10.1016/S2665-9913(20)30121-1

Menachery, V.D., Dinnon, K.H., 3rd, Yount, B.L., Jr., McAnarney, E.T., Gralinski, L.E., Hale, A., Graham, R.L., Scobey, T., Anthony, S.J., Wang, L.*, et al.* (2020). Trypsin Treatment Unlocks Barrier for Zoonotic Bat Coronavirus Infection. J Virol *94*. 10.1128/JVI.01774-19

Menachery, V.D., Yount, B.L., Jr., Debbink, K., Agnihothram, S., Gralinski, L.E., Plante, J.A., Graham, R.L., Scobey, T., Ge, X.Y., Donaldson, E.F.*, et al.* (2015). A SARS-like cluster of circulating bat coronaviruses shows potential for human emergence. Nat Med *21*, 1508-1513. 10.1038/nm.3985

Merrill, J.T., Erkan, D., Winakur, J., and James, J.A. (2020). Emerging evidence of a COVID-19 thrombotic syndrome has treatment implications. Nat Rev Rheumatol *16*, 581-589. 10.1038/s41584-020-0474-5

Millet, J.K., and Whittaker, G.R. (2014). Host cell entry of Middle East respiratory syndrome coronavirus after two-step, furin-mediated activation of the spike protein. Proc Natl Acad Sci U S A *111*, 15214-15219. 10.1073/pnas.1407087111

Nhamo, G., Chikodzi, D., Kunene, H.P., and Mashula, N. (2020). COVID-19 vaccines and treatments nationalism: Challenges for low-income countries and the attainment of the SDGs. Glob Public Health, 1-21. 10.1080/17441692.2020.1860249

Ou, X., Liu, Y., Lei, X., Li, P., Mi, D., Ren, L., Guo, L., Guo, R., Chen, T., Hu, J.*, et al.* (2020). Characterization of spike glycoprotein of SARS-CoV-2 on virus entry and its immune cross-reactivity with SARS-CoV. Nat Commun *11*, 1620. 10.1038/s41467-020-15562-9

Paccaly, A., Frick, A., Rohatagi, S., Liu, J., Shukla, U., Rosenburg, R., Hinder, M., and Jensen, B.K. (2006). Pharmacokinetics of otamixaban, a direct factor Xa inhibitor, in healthy male subjects: pharmacokinetic model development for phase 2/3 simulation of exposure. J Clin Pharmacol *46*, 37-44. 10.1177/0091270005281817

Park, J.H., Her, C., Min, H.K., Kim, D.K., Park, S.H., and Jang, H.J. (2015). Nafamostat mesilate as a regional anticoagulant in patients with bleeding complications during extracorporeal membrane oxygenation. Int J Artif Organs *38*, 595-599. 10.5301/ijao.5000451

Polack, F.P., Thomas, S.J., Kitchin, N., Absalon, J., Gurtman, A., Lockhart, S., Perez, J.L., Perez Marc, G., Moreira, E.D., Zerbini, C.*, et al.* (2020). Safety and Efficacy of the BNT162b2 mRNA Covid-19 Vaccine. N Engl J Med *383*, 2603-2615. 10.1056/NEJMoa2034577

Prado, M., Solano-Trejos, G., and Lomonte, B. (2010). Acute physiopathological effects of honeybee (Apis mellifera) envenoming by subcutaneous route in a mouse model. Toxicon *56*, 1007-1017. 10.1016/j.toxicon.2010.07.005

Qin, C., Zhou, L., Hu, Z., Yang, S., Zhang, S., Chen, M., Yu, H., Tian, D.S., and Wang, W. (2020). Clinical Characteristics and Outcomes of COVID-19 Patients With a History of Stroke in Wuhan, China. Stroke *51*, 2219-2223. 10.1161/STROKEAHA.120.030365

Ramsey, M.L., Nuttall, J., Hart, P.A., and Team, T.I. (2019). A phase 1/2 trial to evaluate the pharmacokinetics, safety, and efficacy of NI-03 in patients with chronic pancreatitis: study protocol for a randomized controlled trial on the assessment of camostat treatment in chronic pancreatitis (TACTIC). Trials *20*, 501. 10.1186/s13063-019-3606-y

Rathore, A.P., Mantri, C.K., Aman, S.A., Syenina, A., Ooi, J., Jagaraj, C.J., Goh, C.C., Tissera, H., Wilder-Smith, A., Ng, L.G.*, et al.* (2019). Dengue virus-elicited tryptase induces endothelial permeability and shock. J Clin Invest *129*, 4180-4193. 10.1172/JCI128426

Riva, L., Yuan, S., Yin, X., Martin-Sancho, L., Matsunaga, N., Pache, L., Burgstaller-Muehlbacher, S., De Jesus, P.D., Teriete, P., Hull, M.V.*, et al.* (2020). Discovery of SARS-CoV-2 antiviral drugs through large-scale compound repurposing. Nature *586*, 113-119. 10.1038/s41586-020-2577-1

Sanjana, N.E., Shalem, O., and Zhang, F. (2014). Improved vectors and genome-wide libraries for CRISPR screening. Nat Methods *11*, 783-784. 10.1038/nmeth.3047

Schmidt, F., Weisblum, Y., Muecksch, F., Hoffmann, H.H., Michailidis, E., Lorenzi, J.C.C., Mendoza, P., Rutkowska, M., Bednarski, E., Gaebler, C.*, et al.* (2020). Measuring SARS-CoV-2 neutralizing antibody activity using pseudotyped and chimeric viruses. J Exp Med *217*. 10.1084/jem.20201181

Shirato, K., Kanou, K., Kawase, M., and Matsuyama, S. (2017). Clinical Isolates of Human Coronavirus 229E Bypass the Endosome for Cell Entry. J Virol *91*. 10.1128/JVI.01387-16

Shrimp, J.H., Kales, S.C., Sanderson, P.E., Simeonov, A., Shen, M., and Hall, M.D. (2020). An Enzymatic TMPRSS2 Assay for Assessment of Clinical Candidates and Discovery of Inhibitors as Potential Treatment of COVID-19. ACS Pharmacol Transl Sci *3*, 997-1007. 10.1021/acsptsci.0c00106

Simmons, G., Bertram, S., Glowacka, I., Steffen, I., Chaipan, C., Agudelo, J., Lu, K., Rennekamp, A.J., Hofmann, H., Bates, P.*, et al.* (2011). Different host cell proteases activate the SARS-coronavirus spike-protein for cell-cell and virus-cell fusion. Virology *413*, 265-274. 10.1016/j.virol.2011.02.020

So, A.D., and Woo, J. (2020). Reserving coronavirus disease 2019 vaccines for global access: cross sectional analysis. BMJ *371*, m4750. 10.1136/bmj.m4750

Song, E., Zhang, C., Israelow, B., Lu-Culligan, A., Prado, A.V., Skriabine, S., Lu, P., Weizman, O.E., Liu, F., Dai, Y.*, et al.* (2021). Neuroinvasion of SARS-CoV-2 in human and mouse brain. J Exp Med *218*. 10.1084/jem.20202135

Stangier, J., and Clemens, A. (2009). Pharmacology, pharmacokinetics, and pharmacodynamics of dabigatran etexilate, an oral direct thrombin inhibitor. Clin Appl Thromb Hemost *15 Suppl 1*, 9S-16S. 10.1177/1076029609343004

Stefely, J.A., Christensen, B.B., Gogakos, T., Cone Sullivan, J.K., Montgomery, G.G., Barranco, J.P., and Van Cott, E.M. (2020). Marked factor V activity elevation in severe COVID-19 is associated with venous thromboembolism. Am J Hematol *95*, 1522-1530. 10.1002/ajh.25979

Straus, M.R., Kinder, J.T., Segall, M., Dutch, R.E., and Whittaker, G.R. (2020). SPINT2 inhibits proteases involved in activation of both influenza viruses and metapneumoviruses. Virology *543*, 43-53. 10.1016/j.virol.2020.01.004

Straus, M.R., and Whittaker, G.R. (2017). A peptide-based approach to evaluate the adaptability of influenza A virus to humans based on its hemagglutinin proteolytic cleavage site. PLoS One *12*, e0174827. 10.1371/journal.pone.0174827

Takeda, K., Matsuno, S., Sunamura, M., and Kakugawa, Y. (1996). Continuous regional arterial infusion of protease inhibitor and antibiotics in acute necrotizing pancreatitis. Am J Surg *171*, 394-398. 10.1016/S0002-9610(97)89617-1

Tang, N., Bai, H., Chen, X., Gong, J., Li, D., and Sun, Z. (2020). Anticoagulant treatment is associated with decreased mortality in severe coronavirus disease 2019 patients with coagulopathy. J Thromb Haemost *18*, 1094-1099. 10.1111/jth.14817

Tang, T., Jaimes, J.A., Bidon, M.K., Straus, M.R., Daniel, S., and Whittaker, G.R. (2021). Proteolytic Activation of SARS-CoV-2 Spike at the S1/S2 Boundary: Potential Role of Proteases beyond Furin. ACS Infect Dis *7*, 264-272. 10.1021/acsinfecdis.0c00701

Tatsumi, K., Antoniak, S., Subramaniam, S., Gondouin, B., Neidich, S.D., Beck, M.A., Mickelson, J., Monroe, D.M., 3rd, Bastarache, J.A., and Mackman, N. (2016). Anticoagulation increases alveolar hemorrhage in mice infected with influenza A. Physiol Rep *4*. 10.14814/phy2.13071

Tsivgoulis, G., Palaiodimou, L., Zand, R., Lioutas, V.A., Krogias, C., Katsanos, A.H., Shoamanesh, A., Sharma, V.K., Shahjouei, S., Baracchini, C.*, et al.* (2020). COVID-19 and cerebrovascular diseases: a comprehensive overview. Ther Adv Neurol Disord *13*, 1756286420978004. 10.1177/1756286420978004

Umapathi, T., Kor, A.C., Venketasubramanian, N., Lim, C.C., Pang, B.C., Yeo, T.T., Lee, C.C., Lim, P.L., Ponnudurai, K., Chuah, K.L.*, et al.* (2004). Large artery ischaemic stroke in severe acute respiratory syndrome (SARS). J Neurol *251*, 1227-1231. 10.1007/s00415-004-0519-8

Walls, A.C., Park, Y.J., Tortorici, M.A., Wall, A., McGuire, A.T., and Veesler, D. (2020). Structure, Function, and Antigenicity of the SARS-CoV-2 Spike Glycoprotein. Cell *181*, 281-292 e286. 10.1016/j.cell.2020.02.058

Wang, Z., Schmidt, F., Weisblum, Y., Muecksch, F., Barnes, C.O., Finkin, S., Schaefer-Babajew, D., Cipolla, M., Gaebler, C., Lieberman, J.A.*, et al.* (2021). mRNA vaccine-elicited antibodies to SARS-CoV-2 and circulating variants. Nature. 10.1038/s41586-021-03324-6

Watanabe, Y., Allen, J.D., Wrapp, D., McLellan, J.S., and Crispin, M. (2020). Site-specific glycan analysis of the SARS-CoV-2 spike. Science *369*, 330-333. 10.1126/science.abb9983

Weisblum, Y., Schmidt, F., Zhang, F., DaSilva, J., Poston, D., Lorenzi, J.C., Muecksch, F., Rutkowska, M., Hoffmann, H.H., Michailidis, E.*, et al.* (2020). Escape from neutralizing antibodies by SARS-CoV-2 spike protein variants. Elife *9*. 10.7554/eLife.61312

Wood, J.P., Silveira, J.R., Maille, N.M., Haynes, L.M., and Tracy, P.B. (2011). Prothrombin activation on the activated platelet surface optimizes expression of procoagulant activity. Blood *117*, 1710-1718. 10.1182/blood-2010-09-311035

Xiao, F., Tang, M., Zheng, X., Liu, Y., Li, X., and Shan, H. (2020). Evidence for Gastrointestinal Infection of SARS-CoV-2. Gastroenterology *158*, 1831-1833 e1833. 10.1053/j.gastro.2020.02.055

Yaghi, S., Ishida, K., Torres, J., Mac Grory, B., Raz, E., Humbert, K., Henninger, N., Trivedi, T., Lillemoe, K., Alam, S.*, et al.* (2020). SARS-CoV-2 and Stroke in a New York Healthcare System. Stroke *51*, 2002-2011. 10.1161/STROKEAHA.120.030335

Zaidel, E.J., Leng, X., Adeoye, A.M., Hakim, F., Karmacharya, B., Katbeh, A., Neubeck, L., Partridge, S., Perel, P., Huffman, M.D.*, et al.* (2020). Inclusion in the World Health Organization Model List of Essential Medicines of Non-Vitamin K Anticoagulants for Treatment of Non-Valvular Atrial Fibrillation: A Step Towards Reducing the Burden of Cardiovascular Morbidity and Mortality. Glob Heart *15*, 52. 10.5334/gh.608

Zang, R., Gomez Castro, M.F., McCune, B.T., Zeng, Q., Rothlauf, P.W., Sonnek, N.M., Liu, Z., Brulois, K.F., Wang, X., Greenberg, H.B.*, et al.* (2020). TMPRSS2 and TMPRSS4 promote SARS-CoV-2 infection of human small intestinal enterocytes. Sci Immunol *5*. 10.1126/sciimmunol.abc3582

Zhou, F., Yu, T., Du, R., Fan, G., Liu, Y., Liu, Z., Xiang, J., Wang, Y., Song, B., Gu, X., *et al.* (2020). Clinical course and risk factors for mortality of adult inpatients with COVID-19 in Wuhan, China: a retrospective cohort study. Lancet *395*, 1054-1062. 10.1016/S0140-6736(20)30566-3

Zhou, Y., Vedantham, P., Lu, K., Agudelo, J., Carrion, R., Jr., Nunneley, J.W., Barnard, D., Pohlmann, S., McKerrow, J.H., Renslo, A.R., *et al.* (2015). Protease inhibitors targeting coronavirus and filovirus entry. Antiviral Res *116*, 76-84. 10.1016/j.antiviral.2015.01.011

Zuo, Y., Estes, S.K., Ali, R.A., Gandhi, A.A., Yalavarthi, S., Shi, H., Sule, G., Gockman, K., Madison, J.A., Zuo, M., *et al.* (2020). Prothrombotic autoantibodies in serum from patients hospitalized with COVID-19. Sci Transl Med *12*. 10.1126/scitranslmed.abd3876

Figure 1. Coagulation factors cleave SARS-CoV-2 Spike.

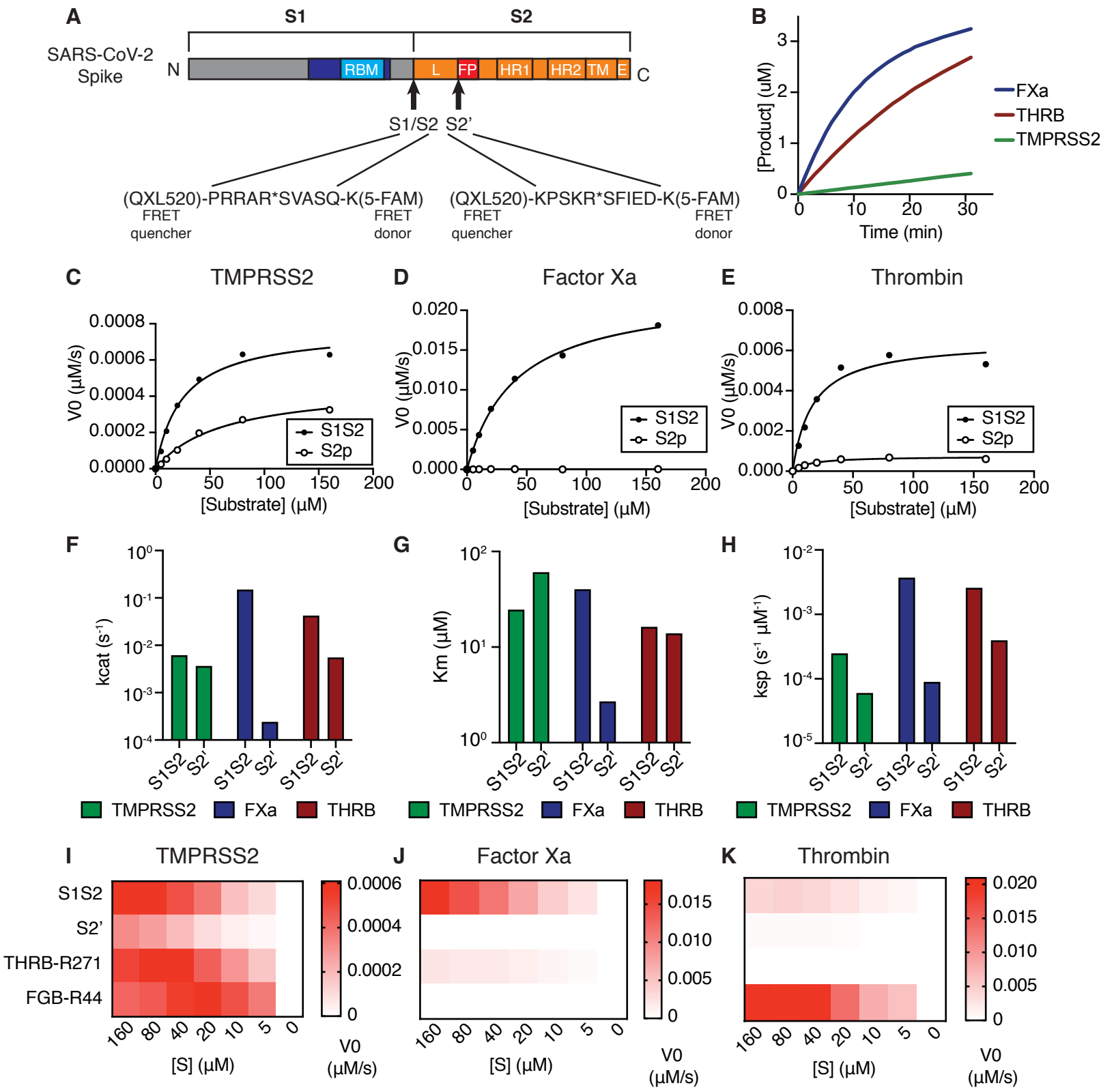

Table 1. Kinetics of SARS-CoV-2 Spike peptide substrate cleavage.

Enzyme	Substrate	V_{max} (μM/s)	k_{cat} (s^{-1})	K_m (μM)	K_{sp} (s^{-1} μM^{-1})
TMPRSS2	S1/S2	7.71E-04	6.17E-03	24.71	2.50E-04
TMPRSS2	S2'	4.60E-04	3.68E-03	60.94	6.04E-05
Factor Xa	S1/S2	2.24E-02	1.79E-01	40.35	4.43E-03
Factor Xa	S2'	3.04E-05	2.43E-04	2.711	8.97E-05
Thrombin	S1/S2	6.50E-03	5.20E-02	16.34	3.18E-03
Thrombin	S2'	7.34E-04	5.87E-03	13.98	4.20E-04

Figure 2. Factor Xa and thrombin facilitate SARS-CoV-2 spike mediated entry.

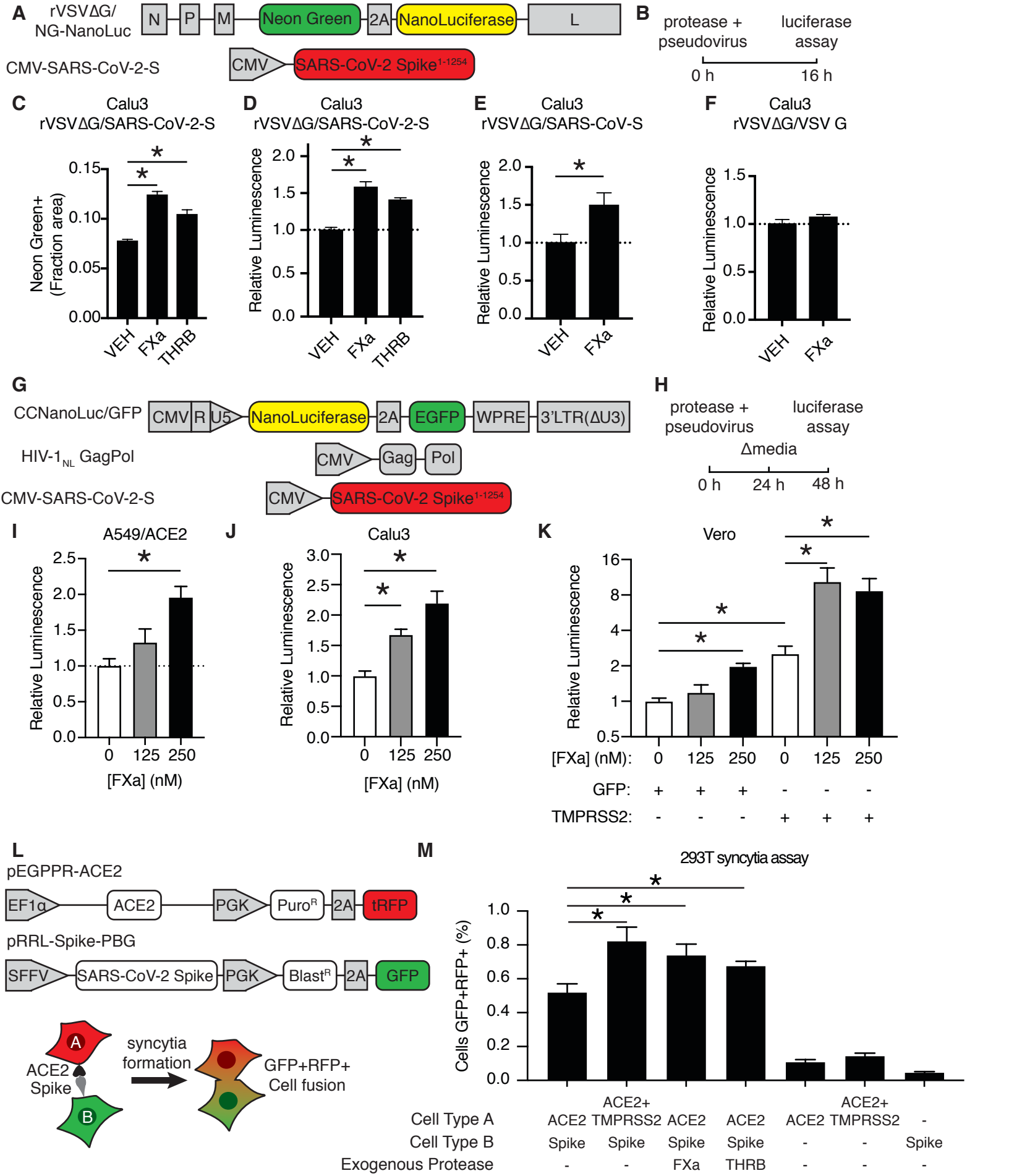

Figure 3. Anticoagulant serine protease inhibitors suppress SARS-CoV-2 entry via inhibition of TMPRSS2.

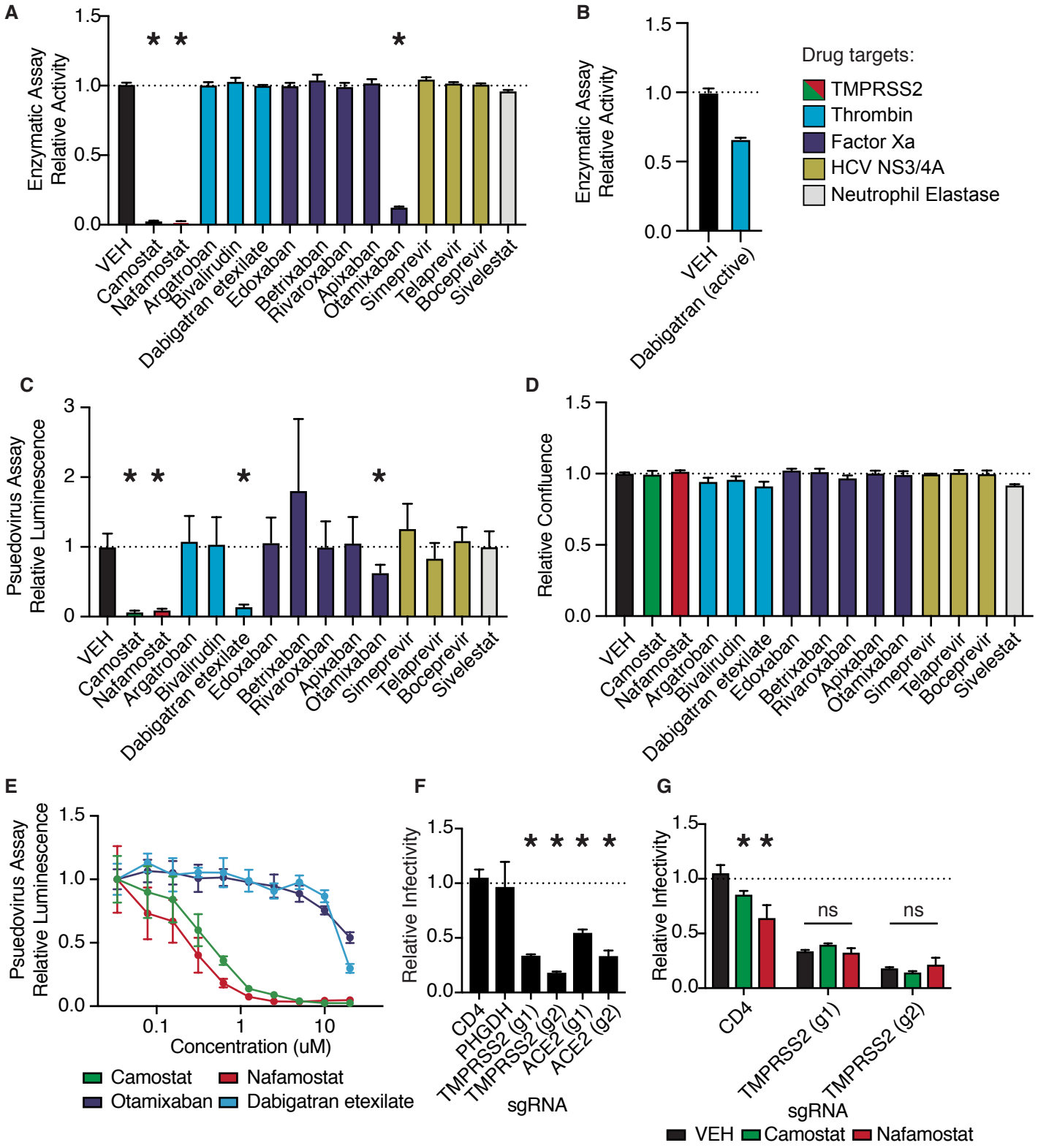

Figure 4. Nafamostat broadly inhibits cleavage of Spike peptides by both coagulation factors and transmembrane serine proteases.

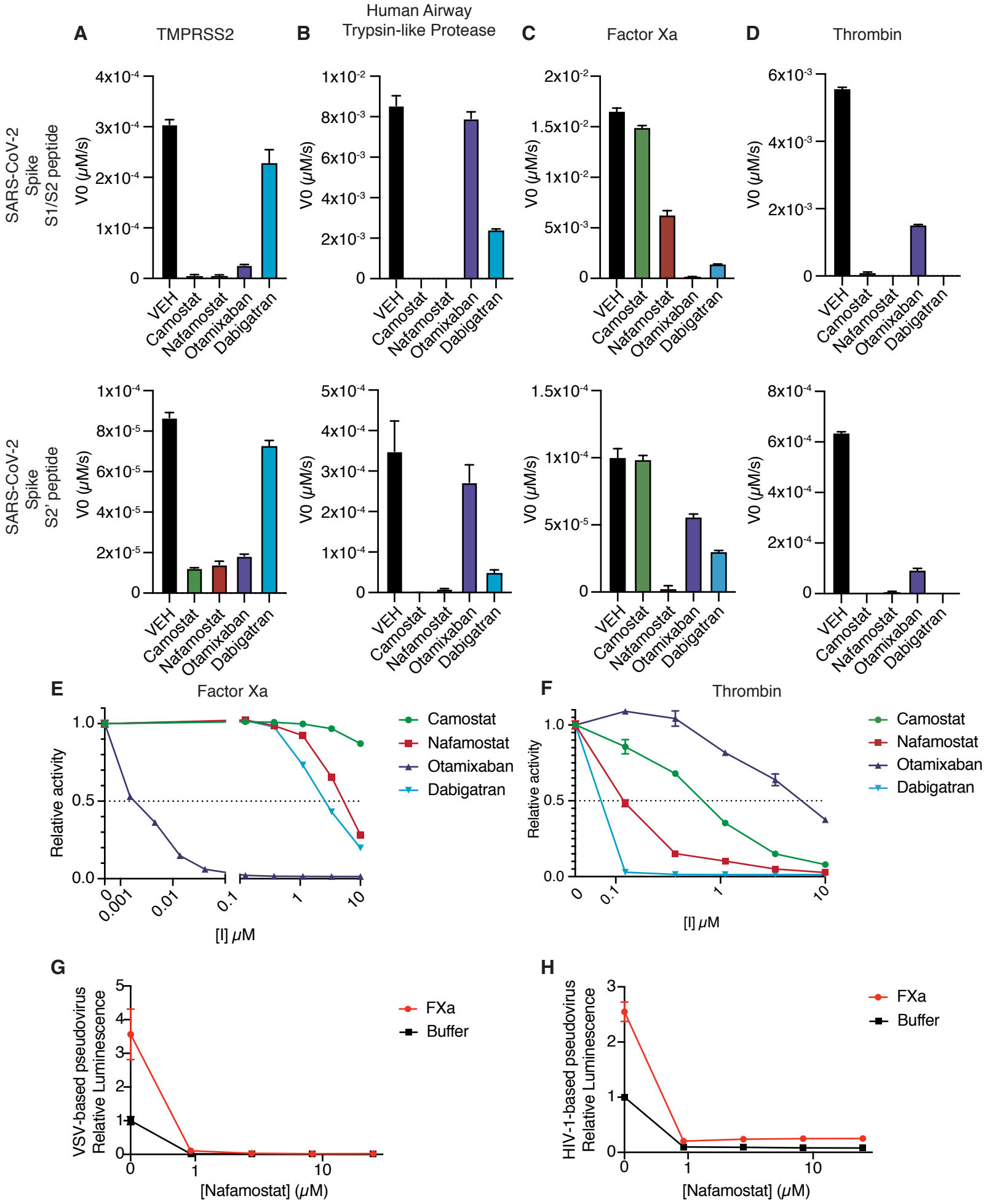

Supplementary Figure 1. Optimization of FRET enzymatic assay.

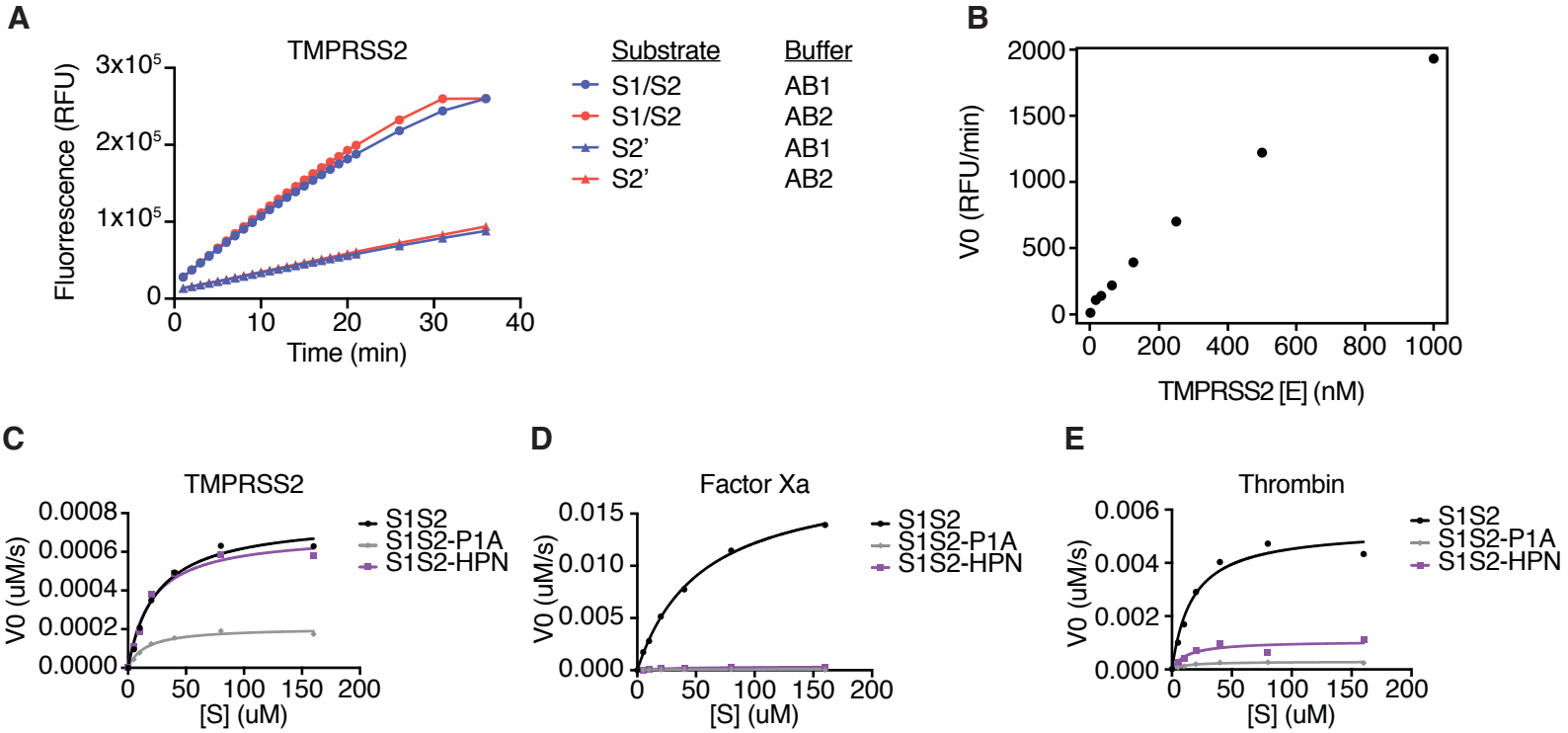

F

Peptide	Sequence (QXL520-X_{10}-K(5-FAM)-NH2)
S1S2	PRRAR^SVASQ
S2'	KPSKR^SFIED
THRB-R271	AIEGR^TATSE
FGB-R44	FFSAR^GHRPL
S1S2-P1A	PRRAA^SVASQ
S1S2-HPN	PSQAR^SVASQ

Supplementary Figure 2. Further characterization of SARS-CoV-2 pseudovirus.

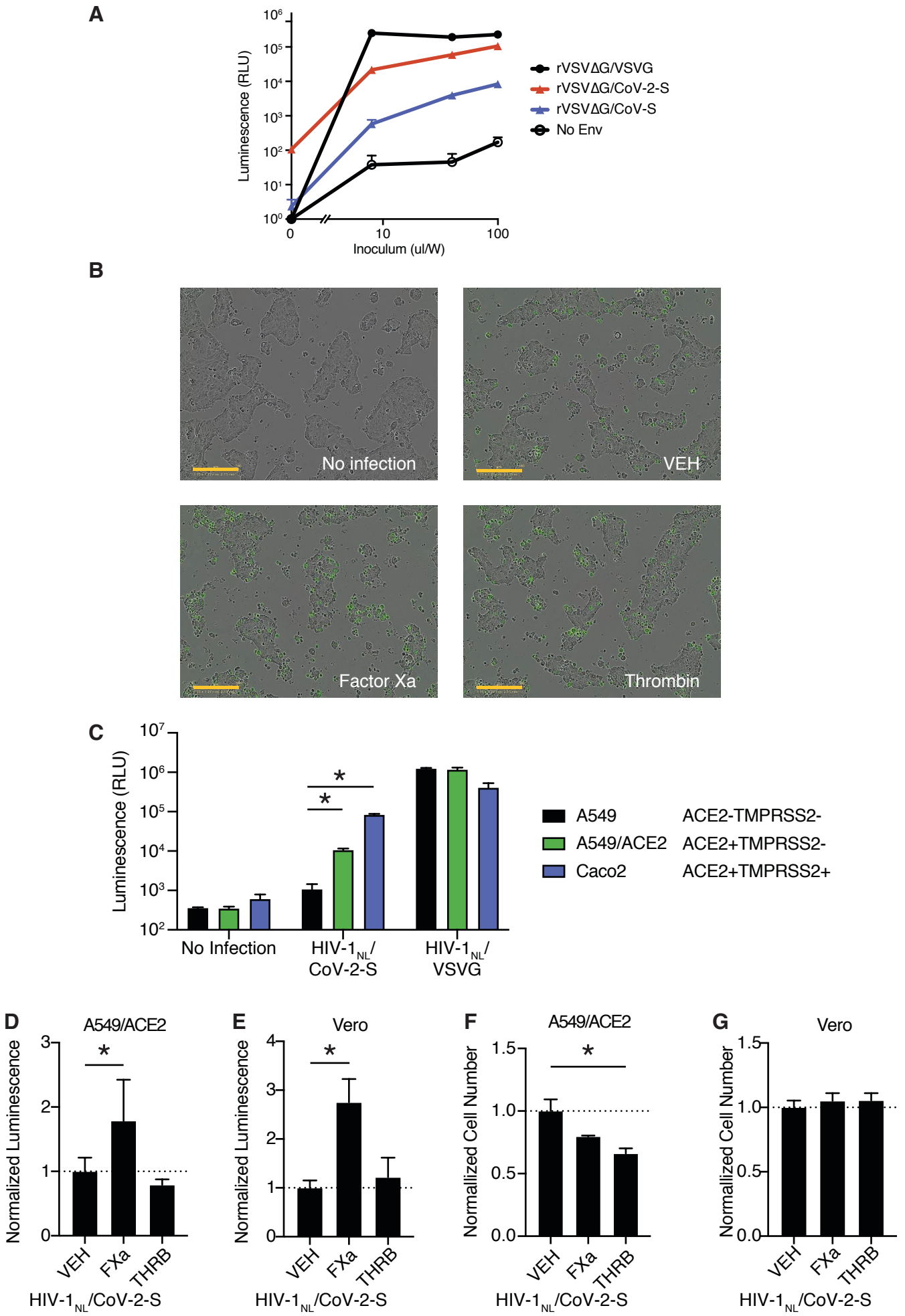

Supplementary Figure 3. Further characterization of antiviral activity of serine protease inhibitors.

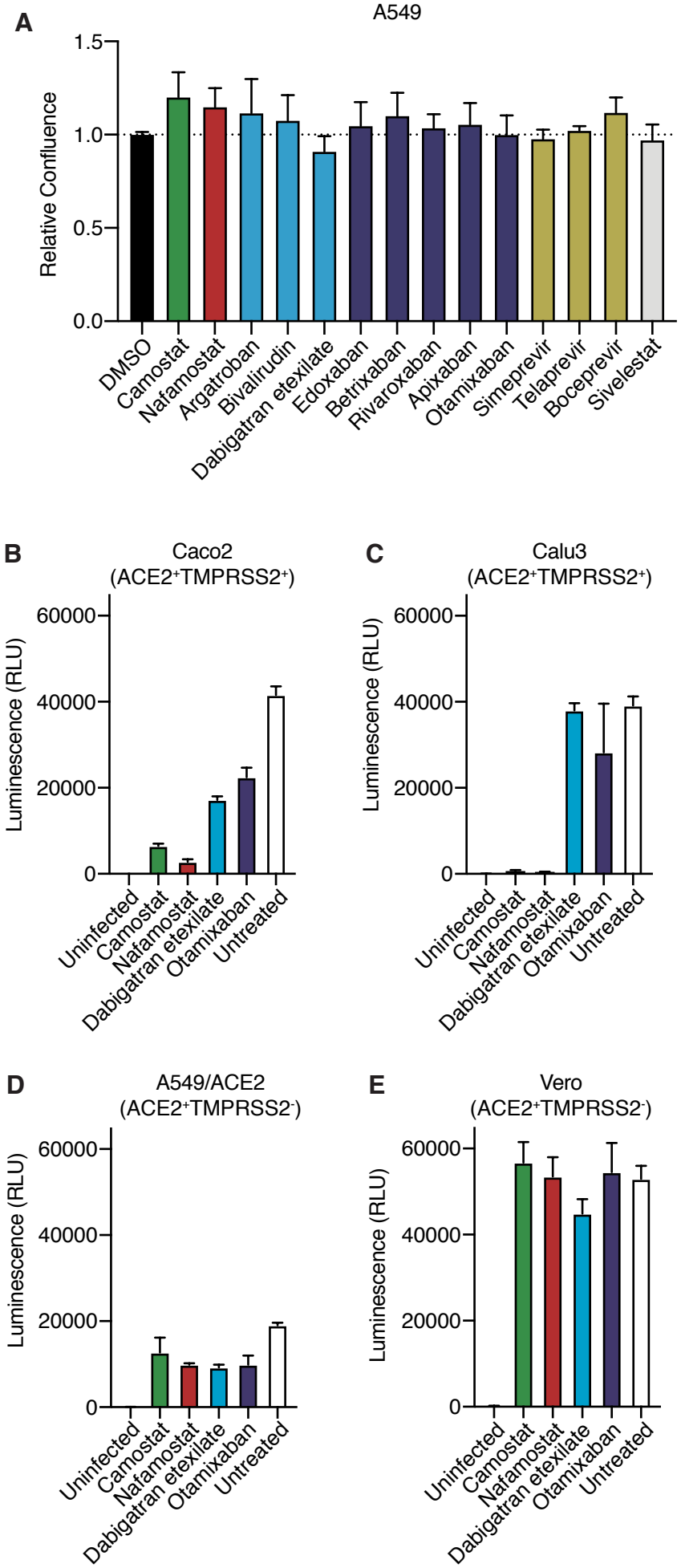

Supplementary Figure 4. Evidence of CRISPR knockout efficiency.

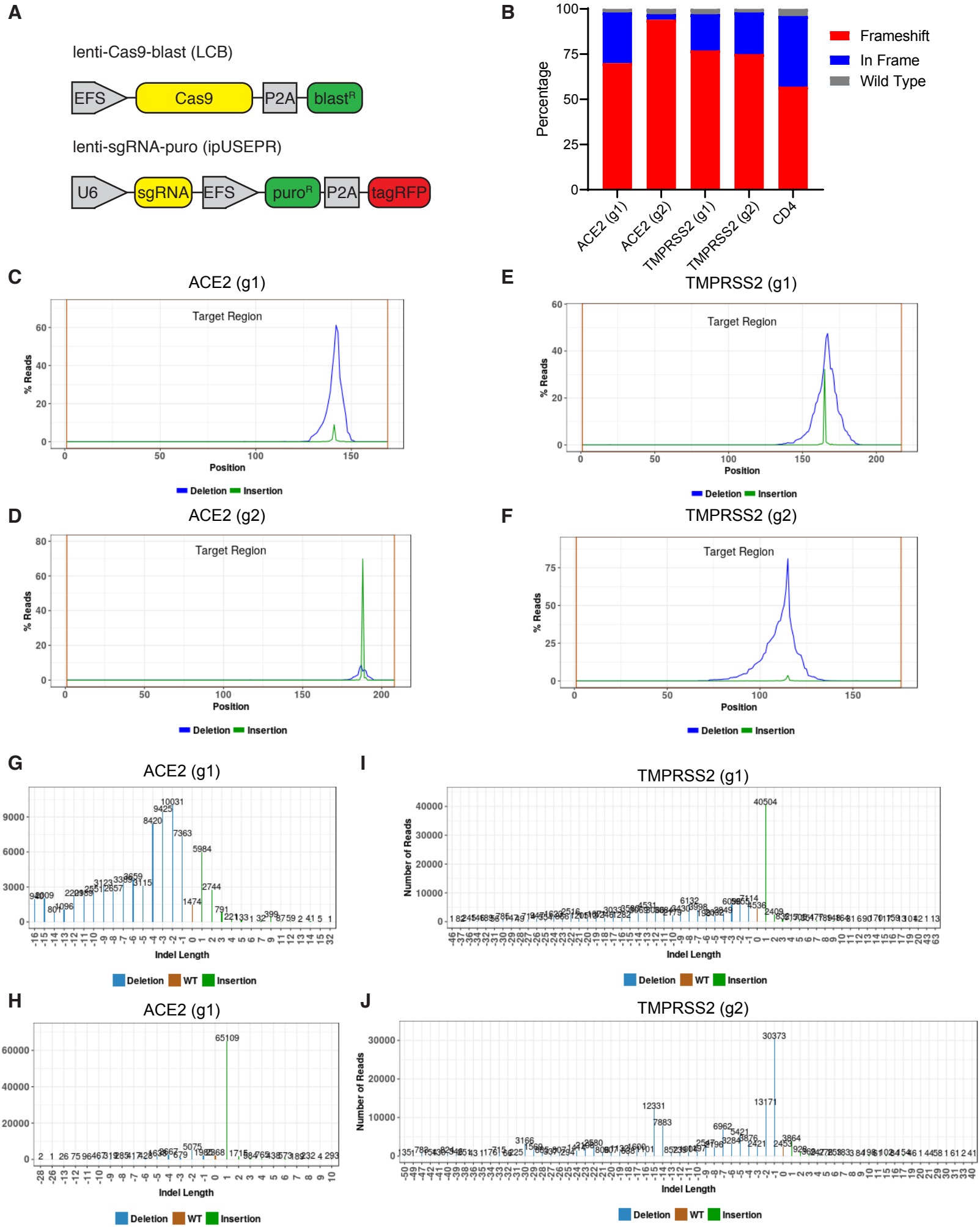
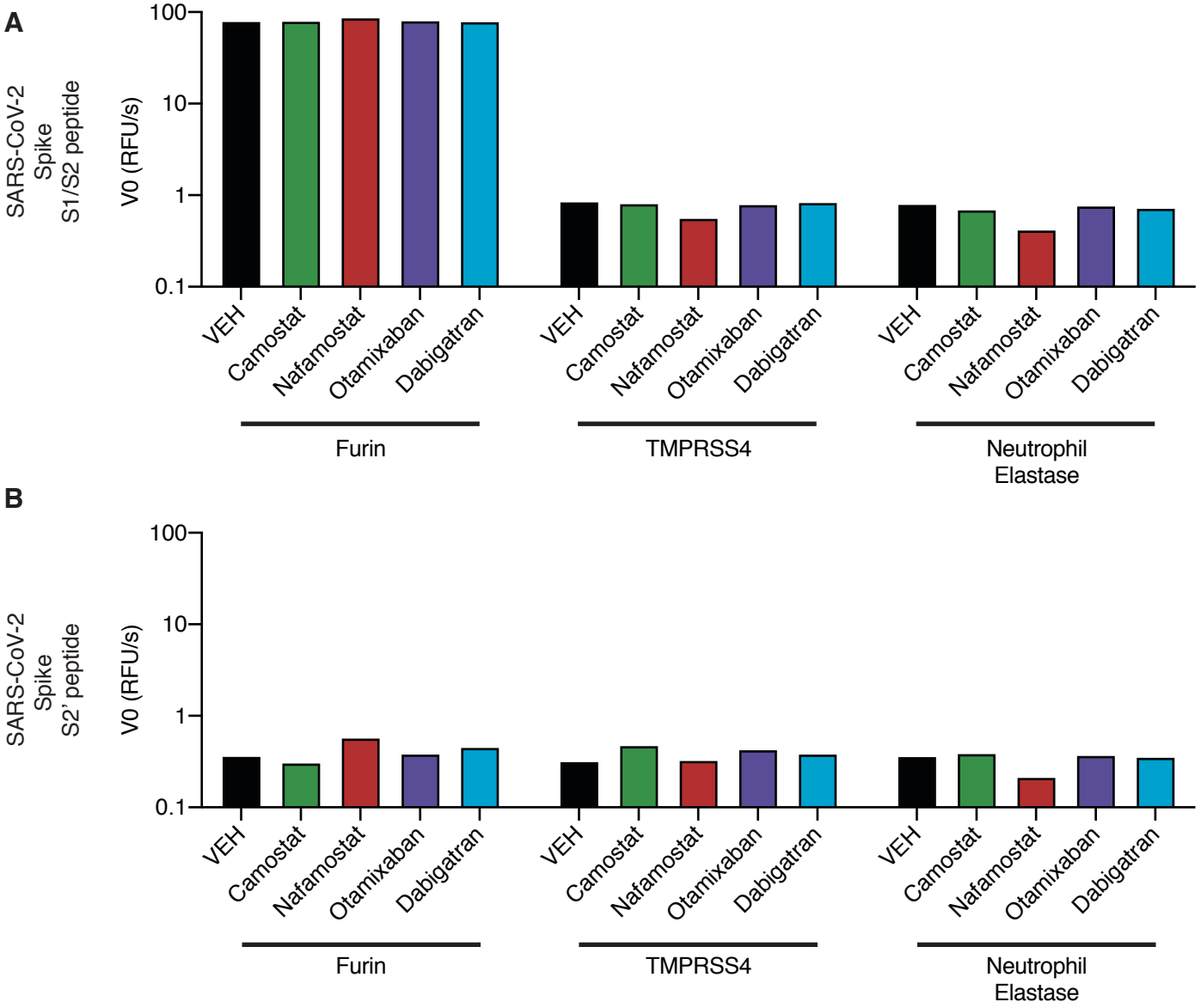
Supplementary Figure 5. Activity of candidate inhibitors against other proteases.